JOC Featured Article

Toward Multistation Rotaxanes Using Metalloporphyrin Coordination Templating

Kathleen M. Mullen and Maxwell J. Gunter*

Department of Chemistry, School of Science and Technology, University of New England, Armidale, NSW 2351, Australia

mgunter@une.edu.au

Received February 10, 2008

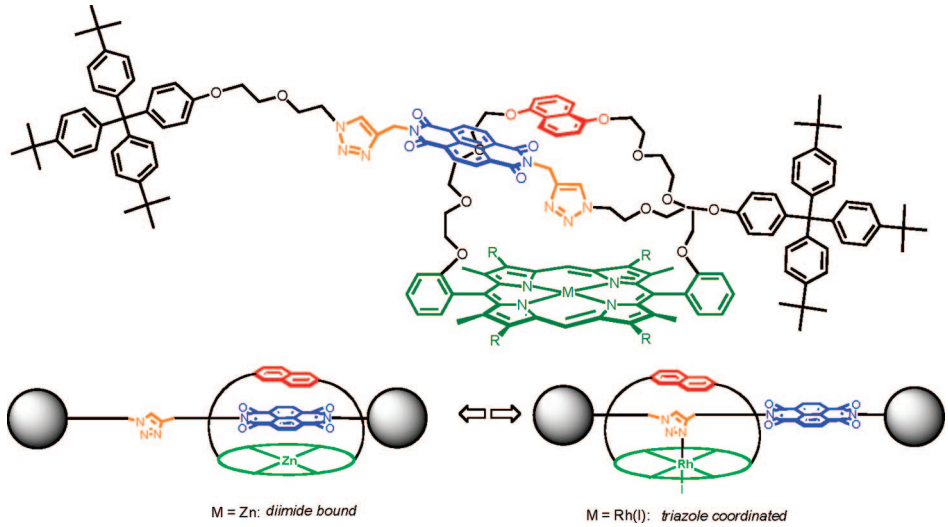

This paper describes some approaches toward the templated synthesis of rotaxanes incorporating strapped metalloporphyrin moieties as the shuttle unit, with the thread component containing both a neutral diimide "station" and a functionalized pyridine moiety, the latter acting not only as a template but also as a second binding motif. In the first instance, the use of appropriately 3,5-difunctionalized pyridine esters and naphthoquinol-strapped rhodium(III) chloride porphyrins in a stoppering approach to rotaxanes produced only unlinked components: the flexibility of the strap allowed sufficient room for the potential thread unit to bind on the same face of the porphyrin as the strap, while not being interlocked through it. An alternative strategy involving a 1,3-dipolar cycloaddition reaction (a "click" reaction) between azides and alkynes, producing triazole linkers in the thread component of rotaxanes, was more successful. Both porphyrinic (zinc, free base, and rhodium(III) derivatives) and crown ether rotaxanes were successfully produced, with multifunctional (triazole and naphthodiimide) thread units. The potential for molecular motion through the use of stimuli such as acid, solvent, and competing ligands was investigated, with limited success. The same cycloaddition methodology was extended to pyridine-templated analogues of the thread components in the Rh(III)-strapped porphyrins, but again, only unlinked thread and porphyrin shuttle units were produced.

Introduction

Although many types of supramolecular entities, such as molecular arrays,[1] knots,[2] cages,[3] and helicates,[3] can be incorporated into both simple dynamic systems, and even more advanced supramolecular devices such as molecular muscles[4,5] and molecular elevators,[6,7] the potential of utilizing "switchable" catenanes and rotaxanes is well-recognized. Incorporation of two or more nondegenerate binding sites in either catenanes or

(1) Burrell, A. K.; Officer, D. L.; Plieger, P. G.; Reid, D. C. W. *Chem. Rev.* **2001**, *101*, 2751–2796.

(2) Reuter, C.; Schmieder, R.; Vogtle, F. *Pure Appl. Chem.* **2000**, *72*, 2233–2241.

10.1021/jo800276w CCC: $40.75 © 2008 American Chemical Society
Published on Web 04/08/2008

rotaxanes can afford the possibility of controlled motion through either translocation (shuttling) of the macrocyclic ring in rotaxanes or pirouetting or co-rotation of the rings in catenane or rotaxanes. To this end, multiple functionalities have been incorporated into rotaxanes and catenanes, and examples of switching between the various co-conformations via chemical,[8] electrochemical,[5,6,9] and photochemical[5,6,10,11] means have been reported.

As the complexity of these systems increases, efficient templating to achieve reasonable yields during their synthesis becomes crucial. Thus we have become interested in using rhodium(III)- and ruthenium(II)-strapped porphyrins as effective templates for a new range of catenanes and rotaxanes.[12] The incorporation of metalloporphyrins as addressable components in a variety of assemblies, particularly, catenanes and rotaxanes, is well-established,[10,13–17] and the rich coordination chemistry of the porphyrin ring has been invoked frequently in templating[18] and self-assembly[1,19] roles for the ordered construction of complex systems.

The coordination properties of simpler, unstrapped ruthenium and rhodium porphyrins have been well-documented,[20–23] and these properties have been used as an advantage in the templated assembly of a variety of supramolecular systems.[17,21,23–26] In each case, the metals are six-coordinate, the fifth ligand being typically CO for Ru(II) and halide (X^-) for Rh(III), and any added nitrogen base L forms stable species [RuP(CO)L] or [RhP(X)L]. In most instances, these systems have incorporated facially symmetrical porphyrins where ligand binding site discrimination has not been an issue.[21,25,27]

We have produced multiporphyrin supramolecular systems using both thermodynamic (metal-ion coordination) and kinetic (covalently attached) principles in both solution studies[14,16,28] and in systems tethered to solid supports.[29] For reversibly assembled rotaxanes, facially symmetrical ruthenium and rhodium porphyrins have functioned as stopper groups. For more advanced systems, we have used a variety of facially differentiated strapped porphyrins for the assembly of a wide range of catenanes, pseudorotaxanes, and rotaxanes.[10,15,16,30–33]

(3) Holliday, B. J.; Mirkin, C. A. *Angew. Chem., Int. Ed.* **2001**, *40*, 2022–2043.

(4) (a) Liu, Y.; Flood, A. H.; Bonvallet, P. A.; Vignon, S. A.; Northrop, B. H.; Tseng, H.-R.; Jeppesen, J. O.; Huang, T. J.; Brough, B.; Baller, M.; Magonov, S.; Solares, S. D.; Goddard, W. A.; Ho, C.-M.; Stoddart, J. F. *J. Am. Chem. Soc.* **2005**, *127*, 9745–9759. (b) Sauvage, J. P. *Chem. Commun.* **2005**, 1507–1510.

(5) Balzani, V.; Credi, A.; Silvi, S.; Venturi, M. *Chem. Soc. Rev.* **2006**, *35*, 1135–1149.

(6) Kay, E. R.; Leigh, D. A.; Zerbetto, F. *Angew. Chem., Int. Ed.* **2007**, *46*, 72–191.

(7) Badjic, J. D.; Ronconi, C. M.; Stoddart, J. F.; Balzani, V.; Silvi, S.; Credi, A. *J. Am. Chem. Soc.* **2006**, *128*, 1489–1499.

(8) (a) Vignon, S. A.; Jarrosson, T.; Iijima, T.; Tseng, H. R.; Sanders, J. K. M.; Stoddart, J. F. *J. Am. Chem. Soc.* **2004**, *126*, 9884–9885. (b) Loeb, S. J. *Chem. Soc. Rev.* **2007**, *36*, 226–235. (c) Elizarov, A. M.; Chiu, S. H.; Stoddart, J. F. *J. Org. Chem.* **2002**, *67*, 9175–9181. (d) Martinez-Díaz, M.-V.; Spencer, N.; Stoddart, J. F. *Angew. Chem., Int. Ed. Engl.* **1997**, *36*, 1904–1907. (e) Ashton, P. R.; Ballardini, R.; Balzani, V.; Fyfe, M. C. T.; Gandolfi, M. T.; Martínez-Díaz, M.-V.; Morosini, M.; Schiavo, C.; Shibata, K.; Stoddart, J. F.; White, A. J. P.; Williams, D. J. *Chem.—Eur. J.* **1998**, *4*, 2332–2341. (f) Ashton, P. R.; Ballardini, R.; Balzani, V.; Baxter, I.; Credi, A.; Fyfe, M. C. T.; Gandolfi, M. T.; Gomez-Lopez, M.; Martinez-Diaz, M.-V.; Piersanti, A.; Spencer, N.; Stoddart, J. F.; Venturi, M.; White, A. J. P.; Williams, D. J. *J. Am. Chem. Soc.* **1998**, *120*, 11932–11942. (g) Ashton, P. R.; Baldoni, V.; Balzani, V.; Credi, A.; Hoffmann, H. D. A.; Martinez-Diaz, M.-V.; Raymo, F. M.; Stoddart, J. F.; Venturi, M. *Chem.—Eur. J.* **2001**, *7*, 3482–3493.

(9) (a) Tian, H.; Wang, Q.-C. *Chem. Soc. Rev.* **2006**, *35*, 361–374. (b) Tseng, H.-R.; Vignon, S. A.; Celestre, P. C.; Perkins, J.; Jeppesen, J. O.; Fabio, A. D.; Ballardini, R.; Gandolfi, M. T.; Venturi, M.; Balzani, V.; Stoddart, J. F. *Chem.—Eur. J.* **2004**, *10*, 155–172. (c) Alteri, A.; Gatti, F. G.; Kay, E. R.; Leigh, D. A.; Martel, D.; Paolucci, F.; Slawin, A. M. Z.; Wong, J. K. Y. *J. Am. Chem. Soc.* **2003**, *125*, 8644–8654.

(10) Gunter, M. J. *Eur. J. Org. Chem.* **2004**, 1655–1673.

(11) (a) Flamigni, L.; Johnston, M. R. *New J. Chem.* **2001**, *25*, 1368–70. (b) Abraham, W.; Grubert, L.; Grummt, U. W.; Buck, K. *Chem.—Eur. J.* **2004**, *10*, 3562–3568. (c) Saha, S.; Stoddart, J. F. *Chem. Soc. Rev.* **2007**, *36*, 77–92. (d) Qu, D.-H.; Wang, Q.-C.; Tian, H. *Org. Lett.* **2004**, *6*, 2085–2088.

(12) (a) Stoddart, J. F. *Acc. Chem. Res.* **2001**, *34*, 410–411. (b) Raymo, F. M.; Stoddart, J. F. In *Supramolecular Organisation and Materials Design*; Jones, W., Rao, C. N. R., Eds.; Cambridge University Press: Cambridge, UK, 2002; pp 332−362. (c) Balzani, V.; Credi, A.; Venturi, M. *Proc. Natl. Acad. Sci. U.S.A.* **2002**, *99*, 4814–4817. (d) Balzani, V.; Credi, A.; Venturi, M. *Chem.—Eur. J.* **2002**, *8*, 5525–5532.

(13) (a) Ballester, P.; Costa, A.; Deya, P. M.; Frontera, A.; Gomila, R. M.; Oliva, A. I.; Sanders, J. K. M.; Hunter, C. A. *J. Org. Chem.* **2005**, *70*, 6616–6622. (b) Andersson, M.; Linke, M.; Chambron, J.-C.; Davidsson, J.; Heitz, V.; Hammarstrom, L.; Sauvage, J.-P. *J. Am. Chem. Soc.* **2002**, *124*, 4347–4362. (c) Andersson, M.; Linke, M.; Chambron, J. C.; Davidsson, J.; Heitz, V.; Sauvage, J. P.; Hammarstrom, L. *J. Am. Chem. Soc.* **2000**, *122*, 3526–3527. (d) Chambron, J.-C.; Heitz, V.; Sauvage, J.-P., In *The Porphyrin Handbook*; Kadish, K. M., Smith, K. M., Guilard, R., Eds.; Academic Press: San Diego, 2000; Vol. 6, pp 1−41. (e) Chichak, K.; Walsh, M. C.; Branda, N. R. *Chem. Commun.* **2000**, 847–848. (f) Chou, J.-H.; Kosal, M. E.; Nalwa, H. S.; Rakow, N. A.; Suslick, K. S., In *The Porphyrin Handbook*; Kadish, K. M., Smith, K. M., Guilard, R., Eds.; Academic Press: San Diego, 2000; Vol. 6, pp 43−131. (g) Coumans, R. G. E.; Elemans, J.; Thordarson, P.; Nolte, R. J. M.; Rowan, A. E. *Angew. Chem., Int. Ed.* **2003**, *42*, 650–654. (h) Linke, M.; Fujita, N.; Chambron, J. C.; Heitz, V.; Sauvage, J. P. *New J. Chem.* **2001**, *25*, 790–796. (i) Maitra, U.; Balasubramaniam, R., In *Supramolecular Organisation and Materials Design*; Jones, W., Rao, C. N. R., Eds.; Cambridge University Press: Cambridge, UK, 2002; pp 363−390. (j) Ogoshi, H.; Mizutani, T.; Hayashi, T.; Kuroda, Y. In *The Porphyrin Handbook*; Kadish, K. M., Smith, K. M., Guilard, R., Eds.; Academic Press: San Diego, 2000; Vol. 6, pp 279−341. (k) Solladie, N.; Chambron, J. C.; Sauvage, J. P. *J. Am. Chem. Soc.* **1999**, *121*, 3684–3692. (l) Flamigni, L.; Heitz, V.; Sauvage, J.-P. *Struct. Bonding* **2006**, *121*, 217–261. (m) Flamigni, L.; Talarico, A. M.; Chambron, J. C.; Heitz, V.; Linke, M.; Fujita, N.; Sauvage, J. P. *Chem.—Eur. J.* **2004**, *10*, 2689–2699.

(14) Gunter, M. J.; Bampos, N.; Johnstone, K. D.; Sanders, J. K. M. *New J. Chem.* **2001**, *25*, 166–173.

(15) Gunter, M. J.; Farquhar, S. M.; Mullen, K. M. *New J. Chem.* **2004**, *28*, 1443–1449.

(16) Gunter, M. J.; Merican, Z. *Supramol. Chem.* **2005**, 1–9.

(17) Ikeda, T.; Asakawa, M.; Shimizu, T. *New J. Chem.* **2004**, *28*, 870–873.

(18) Sanders, J. K. M. *Pure Appl. Chem.* **2000**, *72*, 2265–2274.

(19) (a) Imamura, T.; Fukushima, K. *Coord. Chem. Rev.* **2000**, *198*, 133–156. (b) Hupp, J. T. *Struct. Bonding* **2006**, *121*, 145–165. (c) Iengo, E.; Scandola, F.; Alessio, E. *Struct. Bonding* **2006**, *121*, 105–143. (d) Kobuke, Y. *Struct. Bonding* **2006**, *121*, 49–104. (e) Bouamaied, I.; Coskun, T.; Stulz, E. *Struct. Bonding* **2006**, *121*, 1–47.

(20) (a) Sanders, J. K. M.; Bampos, N.; Clyde-Watson, Z.; Darling, S. L.; Hawley, J. C.; Kim, H.-J.; Mak, C. C.; Webb, S. J. In *The Porphyrin Handbook*; Kadish, K. M., Smith, K. M., Guilard, R., Eds.; Academic Press: New York, 2000; Vol. 3, Chapter 15, p 1. (b) Collman, J. P.; Hutchison, J. E.; Lopez, M. A.; Guilard, R. *J. Am. Chem. Soc.* **1992**, *114*, 8066–8073.

(21) Stulz, E.; Scott, S. M.; Ng, Y. F.; Bond, A. D.; Teat, S. J.; Darling, S. L.; Feeder, N.; Sanders, J. K. M. *Inorg. Chem.* **2003**, *42*, 6564–6574.

(22) (a) Stulz, E.; Maue, M.; Feeder, N.; Teat, S. J.; Ng, Y. F.; Bond, A. D.; Darling, S. L.; Sanders, J. K. M. *Inorg. Chem.* **2002**, *41*, 5255–5268. (b) Stulz, E.; Sanders, J. K. M.; Montalti, M.; Prodi, L.; Zaccheroni, N.; De Biani, F. F.; Grigiotti, E.; Zanello, P. *Inorg. Chem.* **2002**, *41*, 5269–5275.

(23) Stulz, E.; Maue, M.; Scott, S. M.; Mann, B. E.; Sanders, J. K. M. *New J. Chem.* **2004**, *28*, 1066–1072.

(24) (a) Redman, J. E.; Feeder, N.; Teat, S. J.; Sanders, J. K. M. *Inorg. Chem.* **2001**, *40*, 3217–3221. (b) Ikeda, T.; Asakawa, M.; Goto, M.; Nagawa, Y.; Shimizu, T. *Eur. J. Org. Chem.* **2003**, 3744–3751. (c) Stulz, E.; Scott, S. M.; Bond, A. D.; Otto, S.; Sanders, J. K. M. *Inorg. Chem.* **2003**, *42*, 3086–3096. (d) Fukushima, K.; Funatsu, K.; Ichimura, A.; Sasaki, Y.; Suzuki, M.; Fujihara, T.; Tsuge, K.; Imamura, T. *Inorg. Chem.* **2003**, *42*, 3187–3193. (e) Zheng, J. Y.; Tashiro, K.; Hirabayashi, Y.; Kinbara, K.; Saigo, K.; Aida, T.; Sakamoto, S.; Yamaguchi, K. *Angew. Chem., Int. Ed.* **2001**, *40*, 1858–1861.

(25) Redman, J. E.; Feeder, N.; Teat, S. J.; Sanders, J. K. M. *Inorg. Chem.* **2001**, *40*, 2486–2499.

(26) Kim, H. J.; Redman, J. E.; Nakash, M.; Feeder, N.; Teat, S. J.; Sanders, J. K. M. *Inorg. Chem.* **1999**, *38*, 5178–5183.

(27) (a) Webb, S. J.; Sanders, J. K. M. *Inorg. Chem.* **2000**, *39*, 5912–5919. (b) Mak, C. C.; Bampos, N.; Darling, S. I.; Montalti, M.; Prodi, L.; Sanders, J. K. M. *J. Org. Chem.* **2001**, *66*, 4476–4486. (c) Mak, C. C.; Bampos, N.; Sanders, J. K. M. *Chem. Commun.* **1999**, *21*, 1085–1086. (d) Kim, H. J.; Bampos, N.; Sanders, J. K. M. *J. Am. Chem. Soc.* **1999**, *121*, 8120–8121.

(28) (a) Kieran, A. L.; Pascu, S. I.; Jarrosson, T.; Gunter, M. J.; Sanders, J. K. M. *Chem. Commun.* **2005**, 1842–1844. (b) Johnstone, K. D.; Yamaguchi, K.; Gunter, M. J. *Org. Biomol. Chem.* **2005**, *3*, 3008–3017.

(29) (a) Johnstone, K. D.; Bampos, N.; Sanders, J. K. M.; Gunter, M. J. *Chem. Commun.* **2003**, 1396–1397. (b) Johnstone, K. D.; Bampos, N.; Sanders, J. K. M.; Gunter, M. J. *New J. Chem.* **2006**, *30*, 861–867.

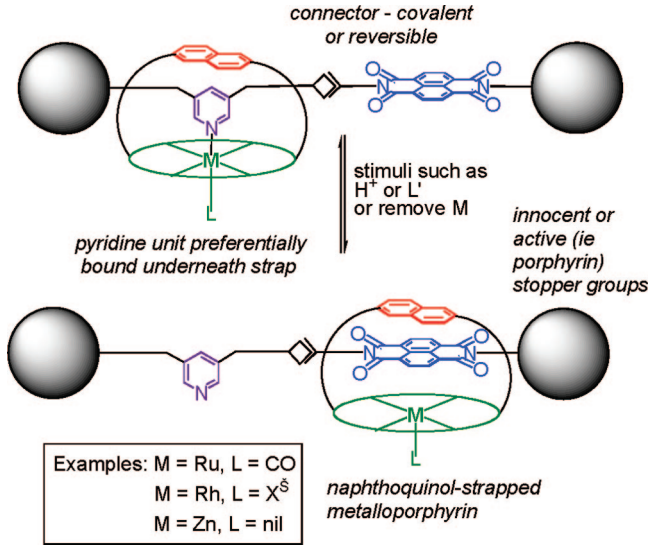

FIGURE 1. Templated rotaxane formation utilizing strong pyridine/metalloporphyrin coordination and a neutral naphthodiimide unit. The pyridine unit must be bound preferentially underneath the strap for effective templating. Protonation of the pyridine, addition of exogenous competing ligand L′, or removal of the metal ion are several of many factors that can be used to reversibly "drive" the rotaxane, causing translational motion of the entrapped macrocycle.

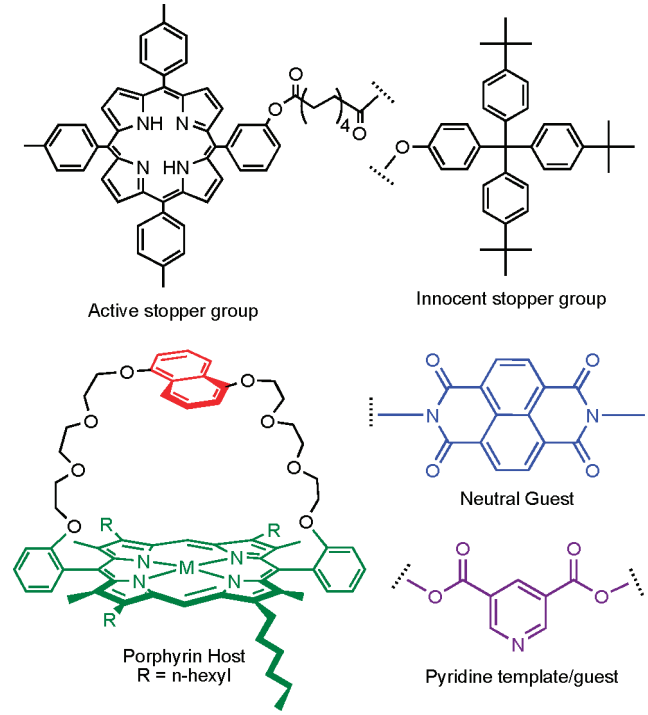

FIGURE 2. Structural components used in this study.

We have addressed the problem of ligand site discrimination in the binding of a variety of pyridine-based ligands to ruthenium(II) and rhodium(III) derivatives of these types of strapped porphyrins.[34] Here it was found that the CO ligand in Ru(II) porphyrins and the X ligand in rhodium(III) porphyrins are surprisingly labile and can coordinate either underneath the strap (inside the cavity) of the strapped porphyrins or on the opposite side (outside). The change in site preference and migration of these counter species can be observed in real time over a period of hours or days,[34] and it was found that there was a subtle thermodynamic balance in the site preference of both the counter ligand (CO or halide) and the chosen pyridine ligands. Thus it was concluded that judicious choice of both strapped porphyrin and ligand(s) is necessary for the construction of more complex supramolecular systems incorporating these design principles.

In our original strategy, we intended to use the templating effect resulting from strong coordination of an appropriately substituted pyridine-based component to produce nonsymmetrical, dual-functionalized, multistation rotaxanes which could be addressed or driven by several different stimuli or inputs, as described in Figure 1.

In this paper, we describe in detail our approaches to the assembly of porphyrin-based rotaxanes based on these principles and the extension of the concepts for an alternative approach to multistation rotaxanes. The various structural components incorporated in this strategy are shown in Figure 2.

Results and Discussion

Pyridine Ligand Templating. Since preliminary studies into the binding of difunctionalized pyridine esters, such as those depicted in Figure 2, indicated only very weak coordination to zinc porphyrins, we favored the use of the stronger Lewis acid ruthenium(II) or rhodium(III) porphyrins for the templated synthetic strategy via a suitably substituted pyridine thread precursor. Alternatively, the incorporation of a diimide moiety as a possible second station could also act as the templating factor, producing interlocked species, as we have shown previously in the successful production of diimide-based porphyrin catenanes.[10,30]

In previous studies, we determined that one of the problems with using ruthenium- or rhodium-strapped porphyrins, and in particular the 3,5-disubstituted pyridine ligands chosen for this investigation, is the tendency of the ligand to migrate to the "outside" position of the strapped porphyrin rather than bind underneath its strap.[34] Nevertheless, it was shown that, in the case of the rhodium(III) chloride porphyrin derivative **1** (Scheme 1), the pyridine ligand coordinated "inside" initially, with only 20% conversion to the outside face of the porphyrin after 3 days at room temperature in the weakly coordinating solvent $CDCl_3$.[34] This provides a viable synthetic route to rotaxanes using this porphyrin/ligand combination, although the choice of reaction conditions is critical to minimize ligand migration; room temperature (or below), noncoordinating solvents such as CH_2Cl_2, and reactions with fast kinetic pathways are required.

In the first instance, assembly of simple rotaxanes by ligand templating was attempted by reaction between pyridine ligand **2** and monosebacoyloxy tetratolyl porphyrin **3** in the presence of the strapped Rh(III) chloride metalloporphyrin **1** (Scheme 1). For further simplicity, a monosubstituted pyridine thread **5** with one end already porphyrin-stoppered was synthesized via a diimide-mediated reaction between pyridine diol **2** and the

(30) Gunter, M. J.; Farquhar, S. M. *Org. Biomol. Chem.* **2003**, *1*, 3450–3457.
(31) Gunter, M. J.; Farquhar, S. M.; Jeynes, T. P. *Org. Biomol. Chem.* **2003**, *1*, 4097–4112.
(32) (a) Gunter, M. J.; Jeynes, T. P.; Turner, P. *Eur. J. Org. Chem.* **2004**, 193–208. (b) Gunter, M. J.; Johnston, M. R *J. Chem. Soc., Perkin Trans. 1* **1994**, 995–1008.
(33) Gunter, M. J.; Hockless, D. C. R.; Johnston, M. R.; Skelton, B. W.; White, A. H. *J. Am. Chem. Soc.* **1994**, *116*, 4810–4823.
(34) Gunter, M. J.; Mullen, K. M. *Inorg. Chem.* **2007**, *46*, 4876–4886.

SCHEME 1

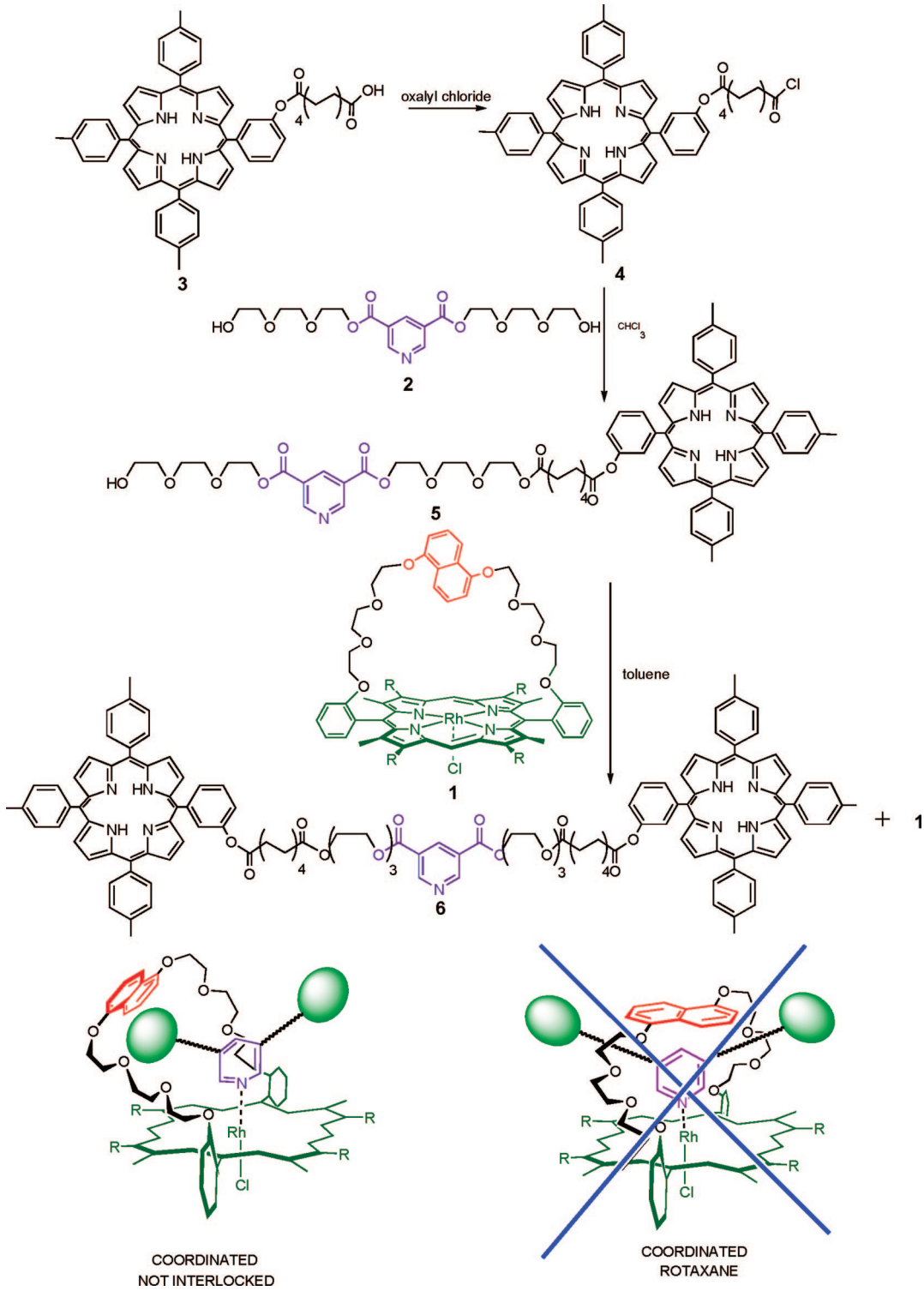

same sebacoyl porphyrin **3** and subjected to the same reaction conditions (Scheme 1). Although the reaction between the thread and stopper units proceeded as expected, no rotaxane was isolated in either case. The ^{1}H NMR of the major rhodium porphyrin product showed clear resonances for bound pyridine protons at 6.23 and 1.83 ppm and the expected integration for a 1:1 rhodium porphyrin macrocycle plus dumbbell complex. However, two separate *meso* proton resonances at 10.30 and 9.95 ppm, as well as split hexyl and methyl side chains peaks, were evident, which is not expected in a symmetrical rotaxane. Furthermore, only one set of peaks for the strapped porphyrin naphthalene aromatic protons (7.07, 6.31, and 5.48 ppm) was evident. This pattern in the strapped porphyrin signals is not consistent with a rotaxane structure, but rather with one in which the central pyridine is coordinated on the same side of the porphyrin as the strap, but where the thread is not interlocked

through the cavity (Scheme 1); a similar situation was observed in previous studies involving coordination of bulky ligands to these strapped porphyrins.[34]

Repeated chromatography of this rhodium porphyrin mixture resulted in slow leaching of the dumbbell from the strapped porphyrin, as expected for a non-interlocked complex as the coordinated pyridine thread is slowly replaced by coordinating solvent (methanol in this case). Indeed, a spectrum identical to the isolated product could be obtained by simple mixing of the isolated thread unit **6** with the strapped rhodium porphyrin **1**. Thus it appears that this templating scheme is thwarted by the flexibility of the strap, despite the apparent success of the pyridine component coordinating to the required inside face of the porphyrin.

Rotaxanes via "Click" Reactions. Thus we abandoned this synthetic strategy for an alternative in which a potentially coordinating unit is produced during the stoppering reaction. One such possibility is provided by an example of a so-called "click" reaction,[35] namely, the Cu(I)-catalyzed Huisgen 1,3-dipolar cycloaddition between alkynes and azides to give 1,2,3-triazoles. This reaction is gaining some currency in the synthesis of supramolecular systems principally because of its mild conditions which favor complexation, preorganization, or templating and result in higher yields of assembled species.[35–38]

However, in our systems, another advantage of using this particular click reaction is that it provides a potential alternative binding site that is introduced directly by the coupling procedure; the triazole unit that is produced could act as a ligand for the metalloporphyrin. So, for example, using a neutral diimide thread component, the triazole formed via the reaction can act as a second functionality or "station" in the final product; multistation rotaxanes and catenanes can thus be easily accessible. (Although this assumes, and we expect, that the 1,2,3-triazole moiety will act as a ligand to a variety of metalloporphyrins, to the best of our knowledge, no previous investigation into the binding of these types of triazoles to metalloporphyrins has been reported.) Shuttling to the diimide might be effected in protonating conditions, by metal-ion removal/replacement or by the presence of a competing ligand (Figure 3). This reaction also may provide mild enough conditions to obtain rhodium chloride rotaxanes or catenanes using pyridine templating, analogous to the concepts and processes discussed above.

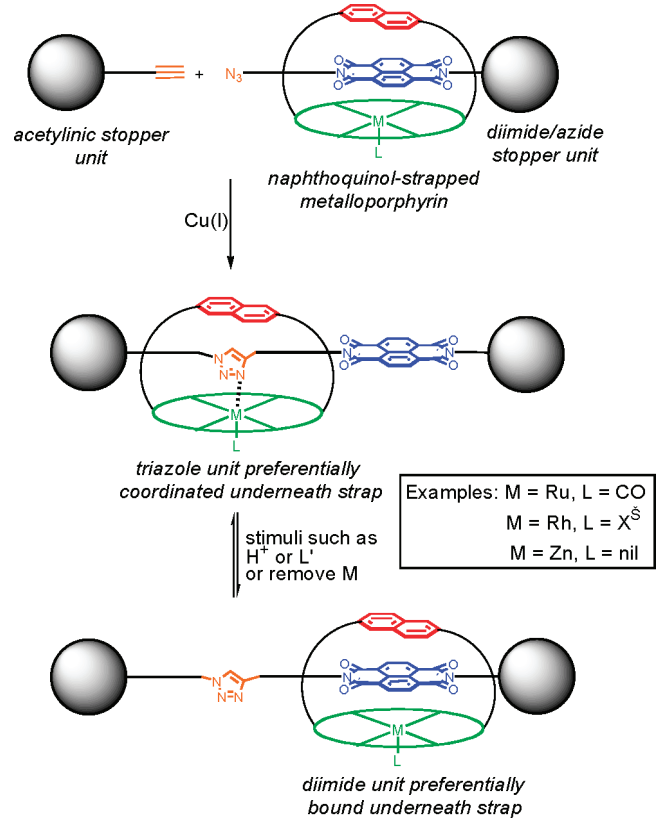

FIGURE 3. Templated formation and dynamics utilizing a click reaction to produce a triazole/metalloporphyrin/naphthodiimide two-station rotaxane. An alternative, but entirely analogous, strategy would involve reaction of a doubly functionalized bisazide diimide with two equivalent acetylinic stopper units. Stimuli for "driving" the rotaxane are as indicated in Figure 1.

Thus it was envisioned that the reaction of an azide-functionalized diimide such as **7** with an alkyne stopper unit **8** in the presence of zinc-strapped porphyrin **9** could yield a two-station rotaxane analogous to that depicted in Figure 3 (Scheme 2). Control experiments in the absence of the strapped porphyrin using the Cu(I) salt $Cu(MeCN)_4BF_4$ (0.1 equiv per alkyne unit **8**) in dry degassed toluene containing excess base (*N*,*N*-diisopropylethylamine, DIPEA, 2 equiv) resulted in the formation of dumbbell **10** in 90% yield (Scheme 2).

However, the parallel reaction in the presence of zinc-strapped porphyrin **9** produced no rotaxane; only dumbbell **10** and recovered porphyrin **9** were isolated from the reaction mixture. This could be explained by the fact that the binding of the structurally similar dihydroxy diimide precursor to **7** (viz. **11**) was shown to be very weak (0.1 M^{-1}). Nevertheless, catenanes incorporating the diimide moiety **12** (Scheme 3), with shorter propynyl substituents in place of the long ethyleneoxy chains, have been made with these strapped porphyrins in up to 60% yields.[30] Although **12** is only sparingly soluble in a variety of suitable solvents, a measurement of its binding constant was carried out by the dilution method (see Supporting Information) and was found to be 800 M^{-1}. (It is likely that this enhanced binding of **12** compared to that of **11** is due to a combination of both the insolubility of the diimide and the possibility of a C−H···O interaction between the relatively acidic hydrogens of the diimide alkyne and the oxygens in the strap of the

(35) (a) Bock, V. D.; Hiemstra, H.; van Maarseveen, J. H. *Eur. J. Org. Chem.* **2006**, *2006*, 51–68. (b) Kolb, H. C.; Finn, M. G.; Sharpless, K. B. *Angew. Chem., Int. Ed.* **2001**, *40*, 2004–2021.

(36) (a) Dichtel, W. R.; Miljanic, O. S.; Spruell, J. M.; Heath, J. R.; Stoddart, J. F. *J. Am. Chem. Soc.* **2006**, *128*, 10388–10390. (b) Miljanic, O. S.; Dichtel, W. R.; Mortezaei, S.; Stoddart, J. F. *Org. Lett.* **2006**, *8*, 4835–4838. (c) Aprahamian, I.; Dichtel, W. R.; Ikeda, T.; Heath, J. R.; Stoddart, J. F. *Org. Lett.* **2007**, *9*, 1287–1290. (d) Trabolsi, A.; Elhabiri, M.; Urbani, M.; Delgado de la Cruz, J. L.; Ajamaa, F.; Solladie, N.; Albrecht-Gary, A. M.; Nierengarten, J. F. *Chem. Commun.* **2005**, 5736–5738. (e) Hahn, U.; Elhabiri, M.; Trabolsi, A.; Herschbach, H.; Leize, E.; Dorsselaer, A. V.; Albrecht-Gary, A. M.; Nierengarten, J. F. *Angew. Chem., Int. Ed.* **1005**, *44*, 5338–5341. (f) Ryu, E. H.; Zhao, Y. *Org. Lett.* **2005**, *7*, 1035–1037. (g) Aucagne, V.; Berna, J.; Crowley, J. D.; Goldup, S. M.; Hanni, K. D.; Leigh, D. A.; Lusby, P. J.; Ronaldson, V. E.; Slawin, A. M. Z.; Viterisi, A.; Walker, D. B. *J. Am. Chem. Soc.* **2007**, *129*, 11950–11963. (h) Kumar, R.; El-Sagheer, A.; Tumpane, J.; Lincoln, P.; Wilhelmsson, L. M.; Brown, T. *J. Am. Chem. Soc.* **2007**, *129*, 6859–6864. (i) Prikhod'ko, A. I.; Durola, F.; Sauvage, J.-P. *J. Am. Chem. Soc.* **2008**, *130*, 448–449. (j) Cabrera, D. G.; Koivisto, B. D.; Leigh, D. A. *Chem. Commun.* **2007**, 4218–4220. (k) Braunschweig, A. B.; Dichtel, W. R.; Miljanic, O. S.; Olson, M. A.; Spruell, J. M.; Khan, S. I.; Heath, J. R.; Stoddart, J. F. *Chem. Asian J.* **2007**, *2*, 634–647. (l) Mobian, P.; Collin, J.-P.; Sauvage, J.-P. *Tetrahedron Lett.* **2006**, *47*, 4907–4909.

(37) Aucagne, V.; Hanni, K. D.; Leigh, D. A.; Lusby, P. J.; Walker, D. B. *J. Am. Chem. Soc.* **2006**, *128*, 2186–2187.

(38) Ornelas, C.; Aranzaes, J. R.; Coutet, E.; Alves, S.; Astruc, D. *Angew. Chem., Int. Ed.* **2007**, *46*, 872–877.

(39) Zhang, Q.; Hamilton, D. G.; Feeder, N.; Teat, S. J.; Goodman, J. M.; Sanders, J. K. M. *New J. Chem.* **1999**, *23*, 897–903.

SCHEME 2

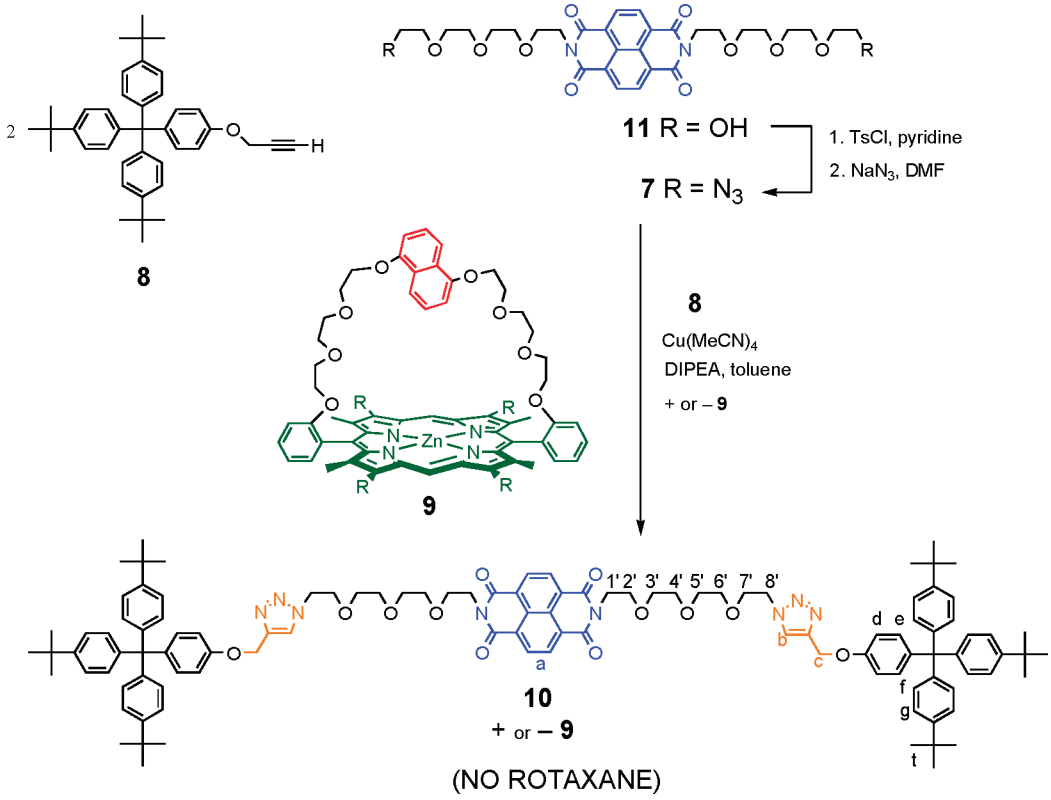

porphyrin.[39] This could account for the fact that catenane reactions using ligand **12** were successful yet rotaxane attempts using diimide **7** were not.)

Thus an attempt was made to create alternative rotaxane **17** using diimide alkyne **12** and blocker azide thread **13**. In this case, three parallel reactions were carried out, one containing just the two components **12** and **13**, a second with the addition of 1 equiv of crown **14**, which not only helps solubilize the diimide but also templates the reaction in favor of the (non-porphyrinic) rotaxane **16**, and third, in the presence of the strapped zinc porphyrin **9**. All other reaction conditions were maintained the same in each case.

Due to the lack of solubility of the diimide, the system without added crown did not reach completion for 8 days, although it did successfully produce good yields of the dumbbell **15** (80%). However, in the reaction in the presence of 1 equiv of crown **14**, not only was the reaction complete after 3 days (assisted by the solubilization of the diimide alkyne **12**) but the mild reaction conditions resulted in the expected dumbbell **15** (46% yield) in addition to good yields of crown rotaxane **16** (43%) (Scheme 3).

The ESI-MS analysis of the crown rotaxane **16** gave peaks at *m/z* 2253.1 $[M + Na]^+$, 2237.1 $[M + Na]^+$, 2215.1 $[M + H]^+$, and 1129.8 $[M/2 + Na]^+$, with very little fragmentation between M^+ and $M/2^+$ peaks, a feature characteristic of interlocked molecules (see Supporting Information, Figure S3).[40]

^{1}H NMR analysis of the crown rotaxane **16** compared to the dumbbell **15** revealed the expected significant upfield shifts in both the naphthodiimide and crown proton resonances (Figure 4). The resonance of the diimide proton a is shifted upfield from 8.74 ppm in the dumbbell **15** to 8.31 ppm in the rotaxane **16** as a result of shielding by the crown. The extent of this shift is comparable to other systems in which this crown is bound around a naphthodiimide thread unit.[14,39,41] Similarly, the crown peaks (α, β, γ) have also been shifted upfield, appearing at 6.77, 6.26, and 5.90 ppm in the bound rotaxane as compared to their typically unbound positions of 7.79, 7.19, and 6.53 ppm, consistent with a cofacial arrangement of crown and diimide aromatic rings. The peak due to the triazole proton c, which is adjacent to the naphthodiimide, also had a small upfield shift of 0.1 ppm, while slight downfield shifts of the b and 1′ peaks are consistent with edge-to-edge deshielding between the triazole and crown rings. In similar diimide−crown catenanes, of Sanders,[39] the protons contiguous to the naphthodiimide moiety showed shielding shifts of around 0.3 ppm and appeared as an AB system. The different splitting pattern and extent of shielding in **16** can be explained by the greater conformational freedom associated with rotaxanes as compared to their typically more restricted catenane counterparts.

NOESY experiments showed clear correlations between the diimide protons a and the protons in the crown ethoxy units (see Supporting Information, Figures S26 and S27; the crown ethoxy proton peaks (1−8) overlap significantly in the ^{1}H NMR spectra, thus the exact protons resulting in the close contact NOE to the diimide proton a cannot be specified), while weaker NOEs were also detected between the naphthodiimide protons and the most upfield crown aromatic proton (α). (This is often not seen in pseudorotaxane systems involving naphthocrowns

(40) Johnston, A. G.; Leigh, D. A.; Nezhat, L.; Smart, J. P.; Deegan, M. D. *Angew. Chem., Int. Ed. Engl.* **1995**, *3411*, 1212–1216.

(41) Hamilton, D. G.; Davies, J. E.; Prodi, L.; Sanders, J. K. M. *Chem.—Eur. J.* **1998**, *4*, 608–620.

SCHEME 3

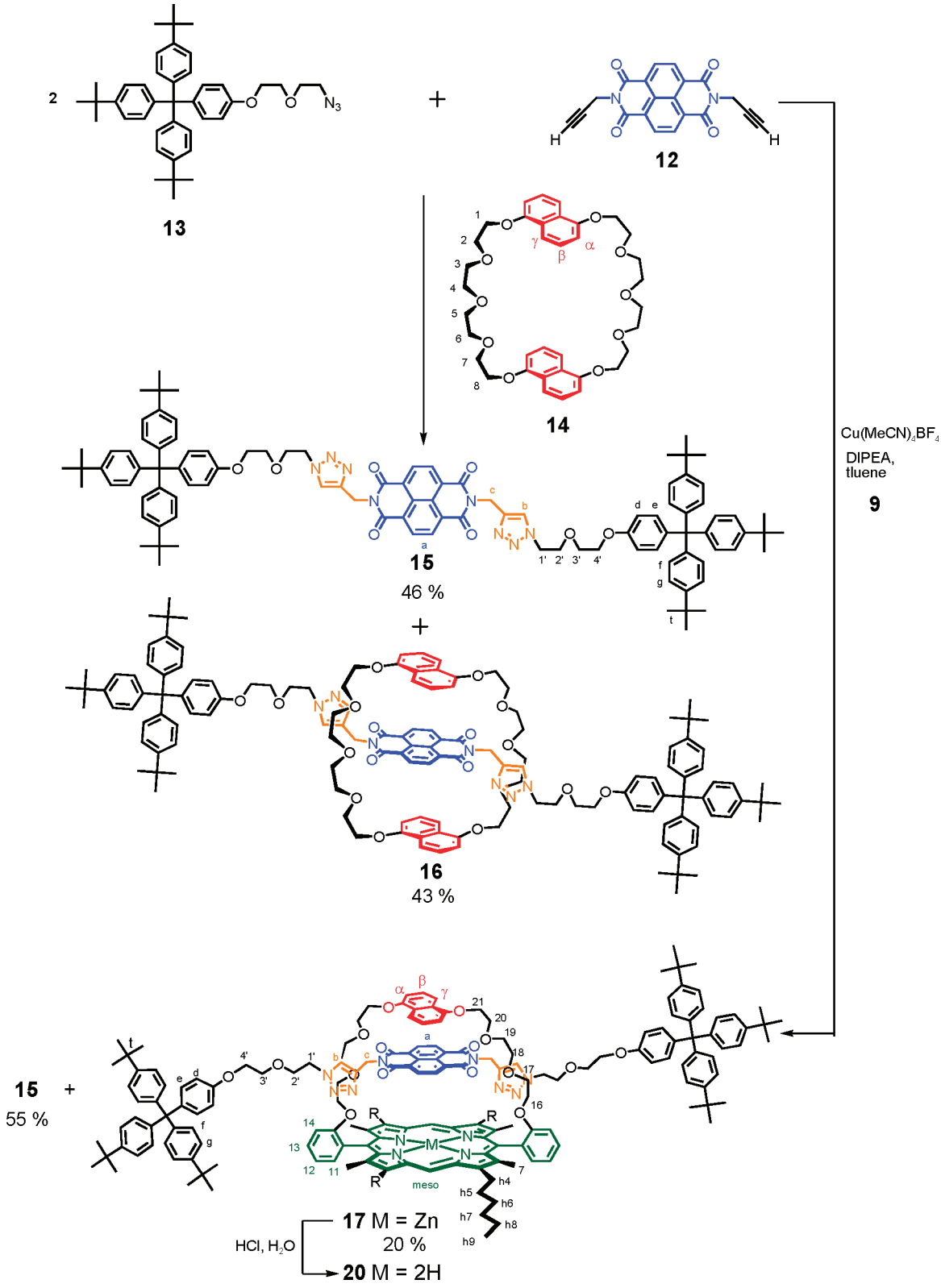

and naphthodiimides; however, due to the permanent interlocking in the rotaxane, close contacts are now more confined and thus detectable.)

In the UV spectrum of the crown rotaxane, there is a charge transfer band at 500 nm (ε 745 M^{-1} cm^{-1}) (see Supporting Information, Figure S28), similar to those observed in related crown−diimide catenane systems which have charge transfer bands between 480 and 530 nm with typical extinction coefficients of 350−880 M^{-1} cm^{-1}.[42]

(42) Hamilton, D. G.; Montalti, M.; Prodi, L.; Fontani, M.; Zanello, P.; Sanders, J. K. M. *Chem.—Eur. J.* **2000**, *6*, 608–617.

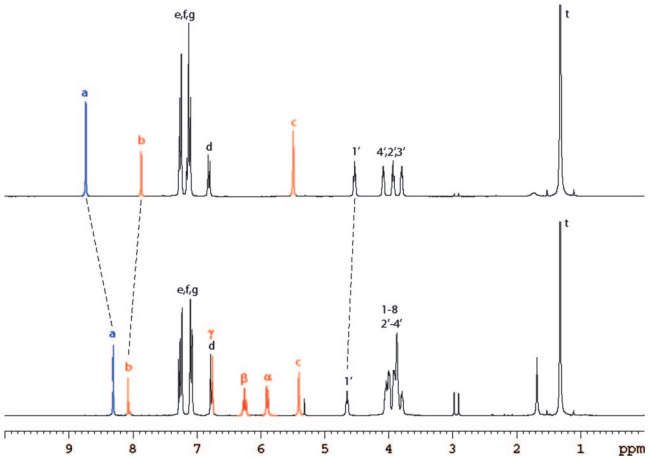

FIGURE 4. ^{1}H NMR comparison of the dumbbell **15** (top) and the corresponding crown rotaxane **16** (bottom). Numbering and lettering refer to those in Scheme 3.

In the third experiment, in the presence of the zinc-strapped porphyrin **9**, after 3 days, both dumbbell **15** (55%) and the porphyrin rotaxane **17** (20%) were isolated (Scheme 3). To date, this is the first successful production of a strapped porphyrin−diimide rotaxane in reasonable yields. Furthermore, the strapped porphyrin starting material that was not entrapped during rotaxane synthesis was recovered intact (75%); although we made no attempts to optimize this reaction, presumably the yields of rotaxane can be enhanced by the use of (recoverable) excess strapped zinc porphyrin.

The ESI-MS analysis of the porphyrin rotaxane **17** gave peaks at *m*/*z* 2916 $[M + H]^+$ and 1459 $[M/2 + H]^+$, with again very little fragmentation between M^+ and $M/2^+$ peaks (see Supporting Information, Figure S29).[40]

^{1}H, COSY, and NOESY NMR studies were used to characterize the zinc porphyrin rotaxane **17** (Figure 5 and Figure S30 in Supporting Information). The diimide resonance a was shifted significantly upfield relative to its position in the uncomplexed dumbbell component ($\Delta\delta$ −2.31 ppm) due to strong shielding by the porphyrin ring. The resonance of triazole protons b at 7.79 ppm was shifted only slightly upfield ($\Delta\delta$ 0.08 ppm), indicating that the triazole is not coordinated to the zinc. This indicates a weaker coordinate covalent binding of the triazole to the zinc than the noncovalent interactions responsible for the binding of the diimide under the naphthoquinol strap of the porphyrin.

Shifts of the naphthoquinol proton peaks (γ, β, α moving from 7.10, 6.39, and 5.38 ppm to 5.87, 5.23, and 4.66 ppm, respectively) and that of the *meso* protons ($\Delta\delta$ −0.36 ppm) are consistent with a structure in which the diimide is located cofacially between the porphyrin and the naphthoquinol aromatic rings. Additionally, the peaks for the porphyrin methylene protons h4 are diastereotopically split, which is to be expected in a structure in which the facial differentiation of the porphyrin is enhanced. Conversely, the resonances for the ethylene protons in the strap of the porphyrin are all shifted downfield, especially protons 18 and 19 ($\Delta\delta$ −1.18 and 1.32 ppm, respectively) and those above and below these positions to a lesser extent, again confirming a cofacial arrangement of the diimide and porphyrin.

Variable temperature ^{1}H NMR measurements down to −40 °C revealed no significant changes in the *meso* diimide a or triazole b proton resonances, indicating that the diimide remains bound at lower temperatures and is not displaced by competitive triazole coordination to the zinc.

Rh(III) Porphyrin Rotaxanes. Such a biased preference for diimide binding over zinc−triazole coordination frustrates the use of this system as a switchable two-station rotaxane. However, by replacement of zinc by a rhodium(III) ion in the strapped porphyrin then, due to its higher affinity for nitrogen ligands, triazole coordination is expected to be more competitive, allowing for switching to the diimide in protonating (or other) conditions. Before proceeding to the corresponding rhodium(III) analogue of the zinc rotaxane **17**, however, some knowledge of possible triazole coordination to rhodium(III) porphyrins was a prerequisite.

Although we could find no literature reports on 1,2,3-triazole metalloporphyrin coordination, there have been examples of the potential of click triazoles to act as ligands in other transition metal complexes.[38,43] It has been shown that in coordination of 1,2,3-triazoles to platinum and palladium metal centers the coordination strength is dependent on their 1- and 4-substituents and typically is comparable to that of simple pyridine-based ligands.[44]

Thus as a simple model for rhodium(III) porphyrin−triazole coordination, the monotriazole thread, **18**, was synthesized from stopper alkyne **8** and stopper azide **13** via the standard click methodology previously discussed.

^{1}H NMR spectra revealed that addition of 1 equiv of rhodium porphyrin **19** to **18** resulted in the complex **19**⊃**18** (see Supporting Information, Figure S35), showing significant upfield shifts in the resonance of the triazole proton b from 7.81 to 5.51 ppm, with that of proton c shifting from 5.13 to 0.27 ppm, indicative of strong triazole coordination to the rhodium porphyrin. In addition to this, the resonances of the stopper aromatic protons d and d′ were also shifted upfield from 6.76 ppm in the monotriazole thread **18** to 6.45 (proton d) and 5.32 ppm (proton d′) in **19**⊃**18** due to shielding by the adjacent porphyrin, which was also responsible for upfield shifts in the signals of the adjacent ethoxy protons (1′−4′). Spectra of a mixture of dumbbell **15** with 2 equiv of iodo-rhodium(III) tetratolyl porphyrin **19** (1 equiv for each triazole) also revealed strong triazole coordination.

Despite these control experiments with monotriazole thread **18** and dumbbell **15** clearly showing triazole coordination to rhodium porphyrins, in the proposed rhodium analogue of the zinc porphyrin rotaxane **17**, only one rhodium porphyrin for two possible coordinating triazole entities is present. A more realistic model, although more complicated, is one in which only 1 equiv of rhodium tetratolyl porphyrin **19** is added to the bistriazole dumbbell **15** (**19**⊃**15**, Figure 6).

^{1}H NMR analysis of such a mixture revealed that, at 30 °C, many of the proton signals for the thread, diimide, and triazole protons were broadened and undetectable, presumably as a result of fast exchange between possible coordinated species. At −20 °C, however, the broadness had resolved and multiple peaks for each of the components were observed (Figure 7). As expected the system was complicated, and signals for three distinct coordination

(43) (a) Chang, K.-C.; Su, I.-H.; Lee, G.-H.; Chung, W.-S. *Tetrahedron Lett.* **2007**, *48*, 7274–7278. (b) David, O.; Maisonneuve, S.; Xie, J. *Tetrahedron Lett.* **2007**, *48*, 6527–6530. (c) Chang, K.-C.; Su, I.-H.; Senthilvelan, A.; Chung, W.-S. *Org. Lett.* **2007**, *9*, 3363–3366. (d) Li, Y.; Huffman, J. C.; Flood, A. H. *Chem. Commun.* **2007**, 2692–2694. (e) Bronisz, R. *Inorg. Chem.* **2005**, *44*, 4463–4465.

(44) Suijkerbuijk, B. M. J. M.; Aerts, B. N. H.; Dijkstra, H. P.; Lutz, M.; Spek, A. L.; van Koten, G.; Gebbink, R. J. M. K. *J. Chem. Soc., Dalton Trans.* **2007**, 1273–1276.

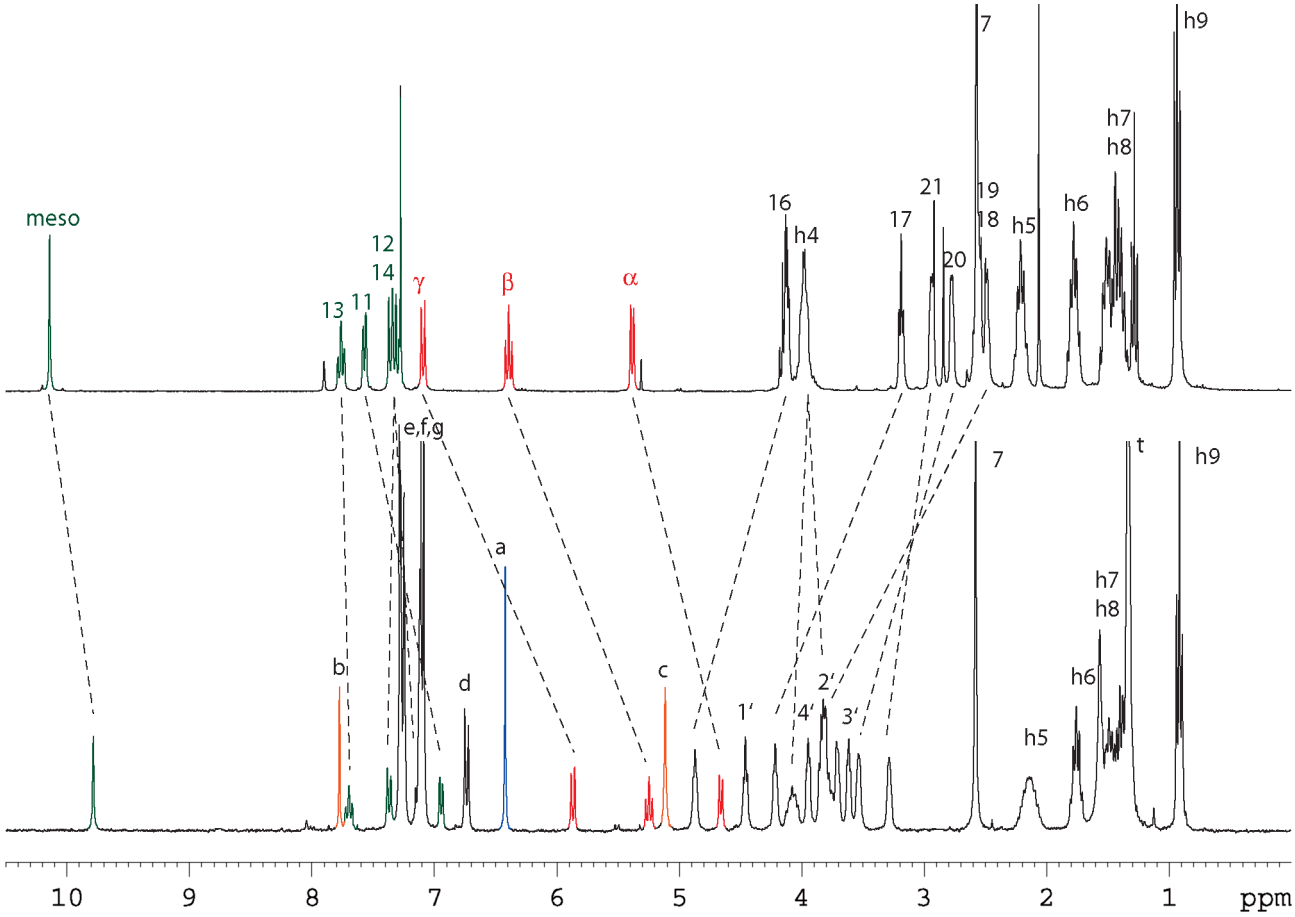

FIGURE 5. ^{1}H NMR spectra of the strapped porphyrin **9** (top) compared to the porphyrin rotaxane **17** (bottom). Numbering and lettering refer to those in Scheme 3.

species were observed, resulting from a statistical mixture containing uncoordinated (**15**), mono- (**19**⊃**15**), and di- (2.**19**⊃**15**) coordinated dumbbell. These could be separated by rationalization of their shifts and by 2-D experiments.

Of particular interest is the monocoordinated species **19**⊃**15**, as in a rhodium rotaxane no unbound or dicoordinated species is expected. This component of the spectrum of the mixture shows complete asymmetry as expected, and at −20 °C, clear peaks for bound (5.40 ppm) and unbound (7.89 ppm) triazole proton b and bound (0.53 ppm) and unbound (5.34 ppm) NCH_2 triazole protons c are evident. In addition to this, and because of the asymmetry, the resonances of the diimide protons a are shifted upfield and split into two doublets at 8.52 and 8.31 ppm due to shielding by the porphyrin, as are the resonances of the stopper aromatic protons at 6.78 and 6.54 ppm and the ethoxy protons (1′−4′) in the thread. This asymmetric pattern could now be used as a model to decipher the ^{1}H NMR spectrum of the proposed rhodium analogue of rotaxane **17**.

Before rhodium could be inserted into the porphyrin rotaxane, the zinc was removed by washing with dilute HCl. ^{1}H NMR analysis of the free base rotaxane **20** (Scheme 3) showed that the rotaxane remained intact. In this free base derivative, the diimide remained bound, as evidenced by the upfield position of the diimide (6.36 ppm) and naphthoquinol (5.88, 5.29, and 4.68 ppm) resonances. Indeed, no significant changes in the NMR chemical shift patterns were observed compared to the zinc-strapped porphyrin rotaxane **17** except for the presence of the porphyrin NH peaks at −4.27 ppm in **20**. These resonances are significantly more upfield than in typical free base porphyrins, which normally appear around −2 to −3 ppm,[31,33] which is further evidence of the diimide being bound in the cavity of the strapped porphyrin in a cofacial arrangement.

Insertion of rhodium into the rotaxane was achieved according to usual procedures[26] to afford the rhodium iodide rotaxane **21** in 40% yield. It appeared that some of the rotaxane material was destroyed during the rhodium insertion, but nevertheless, reasonable quantities of rhodium rotaxane were obtained.

The ESI-MS analysis of the rhodium porphyrin rotaxane **21** showed a major *m*/*z* peak at 3082 representing the $[M + H]^+$ species, with the iodide ligand remaining coordinated to the rhodium metal. Minor peaks at 2954 for the $[M - I]^+$ and 2986 for the $[(M - I) + Na]^+$ were also present (see Supporting Information, Figure S31).

At room temperature, the peaks observed in the ^{1}H NMR spectrum of **21** were broad, indicative of fast exchanging processes. However, at −20 °C, the spectrum had resolved considerably, and two sets of peaks for many of the porphyrin and thread protons were apparent (see Figure 8).

This asymmetry is due to the rhodium porphyrin binding of only one of the two triazole entities present in the thread and is similar to that seen in the monotetratolyl rhodium coordination to dumbbell **15** (viz. **19**⊃**15**) discussed above. At −20 °C, clear peaks for bound (5.02 ppm) and unbound (7.97 ppm) triazole proton b and bound (0.11 ppm) and unbound (5.43 ppm)

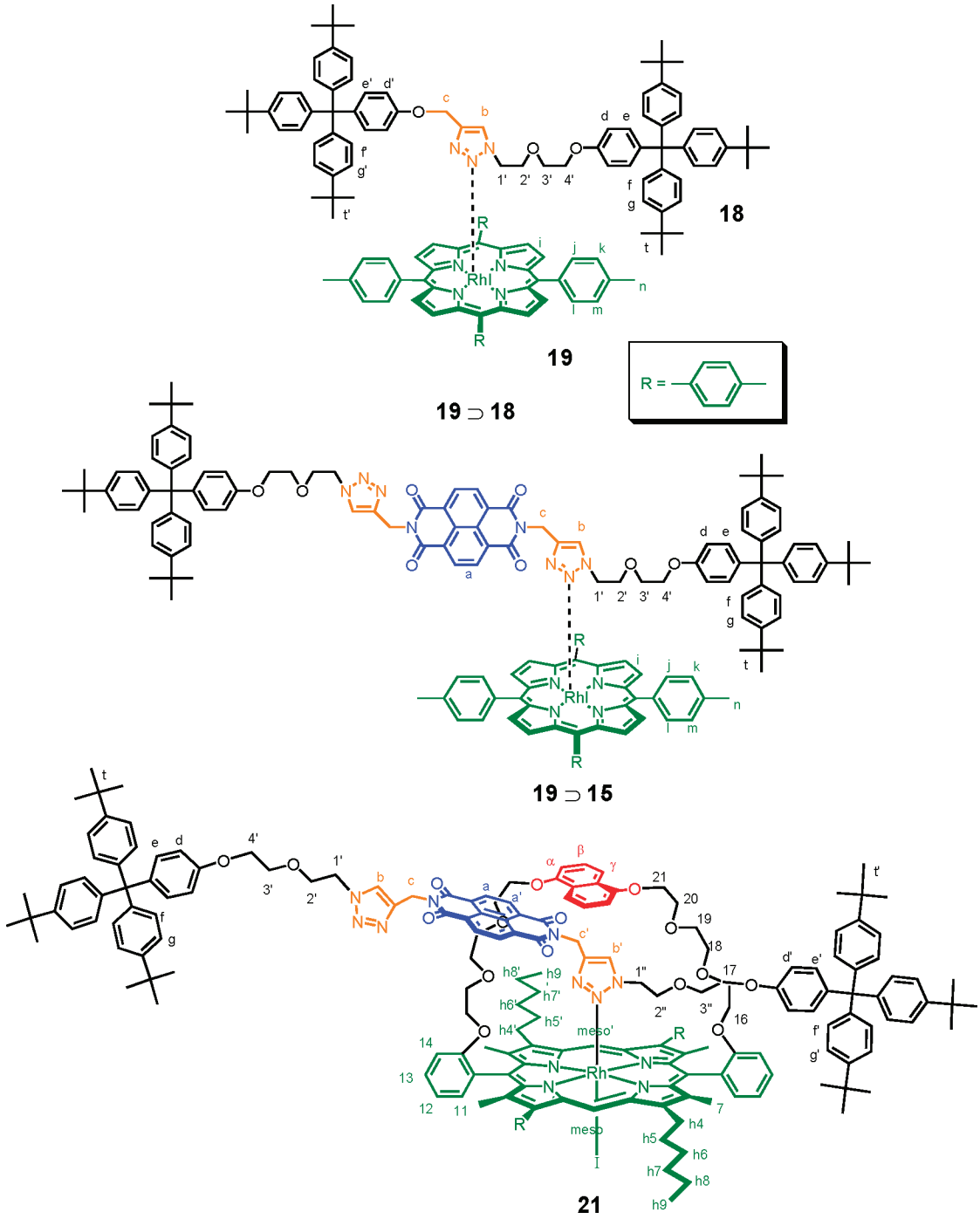

FIGURE 6. Triazole-coordinated Rh(III) porphyrin species discussed in the text. Labelling refers to the NMR spectra illustrated in Figures 5−8.

NCH_2−triazole protons c are evident. The 1:1 ratio confirms that the porphyrin is coordinated to only one of the triazole units of the thread and that the broadness at higher temperatures is probably due to a shuttling process between the two triazoles. Furthermore, the diimide proton resonance a is split into two doublets at 8.31 and 7.88 ppm, as are the stopper aromatic resonances d at 6.62 (end closest to the porphyrin) and 6.82 ppm (furthest from the porphyrin) as a result of the induced asymmetry.

The induced C_2 symmetry is also reflected in paired porphyrin resonances. Thus the peaks for the porphyrin *meso* protons and the methyl and hexyl protons are split into two at −20 °C. However, no asymmetry in the side aromatic protons of the porphyrin or the naphthoquinol aromatic protons in the porphyrin strap is observed, indicating that these are reflected in the perpendicular mirror plane. NOESY experiments clearly show close contacts between the naphthoquinol and the bound triazole peak, confirming coordination of the triazole and that the diimide moiety is thus displaced from the cavity (see Supporting Information, Figures S33 and S34).

Attempted Shuttling Processes. Having fully characterized the rhodium rotaxane **21** and established that the preferred

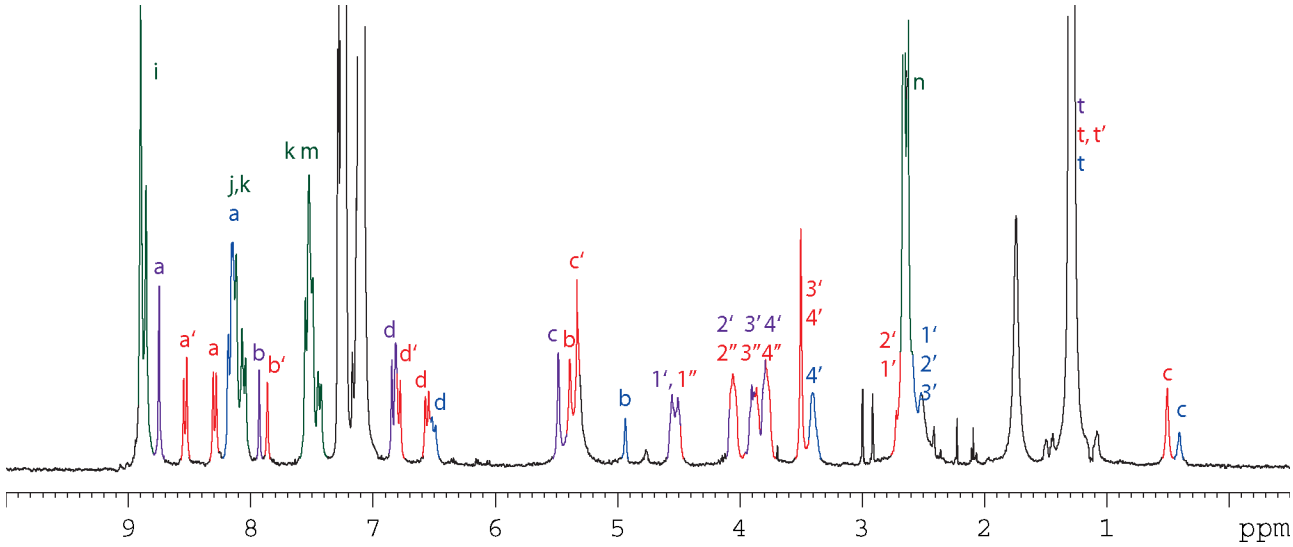

FIGURE 7. [1]H NMR spectrum at −20 °C of a mixture of dumbbell **15** with 1 equiv of rhodium porphyrin **19**. Cyan colors indicate unbound dumbbell **15**; blue colors indicate diporphyrin coordinated dumbbell (2.**19**⊃**15**); and red colors indicate monocoordinated dumbbell (**19**⊃**15**). For the monocoordinated species, two sets of peaks are evident with the coordinated side numbered as above, and the uncoordinated side with additional d′, 1″, etc.

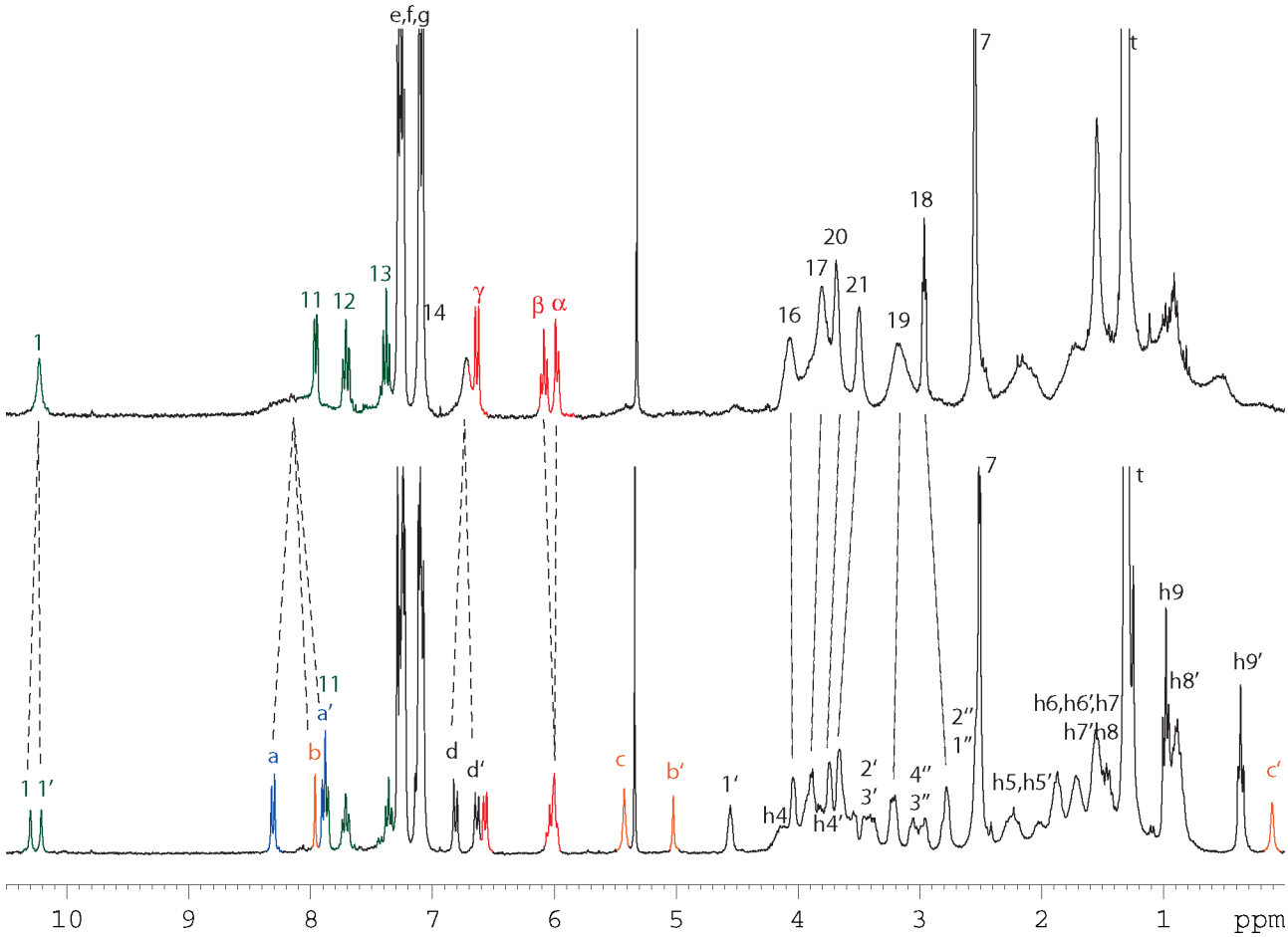

FIGURE 8. [1]H NMR spectra of the rhodium rotaxane **21** at 30 °C (top) and −20 °C (bottom). Numbering and lettering refer to those shown in Figure 6.

conformation is with coordinated triazole rather than bound diimide (quite the opposite of that observed for the zinc derivative), various methods for initiating a reversible switching process were investigated. A set of conditions under which the triazole coordination can be interrupted to allow the diimide to bind inside the cavity is required for a controlled translational movement.

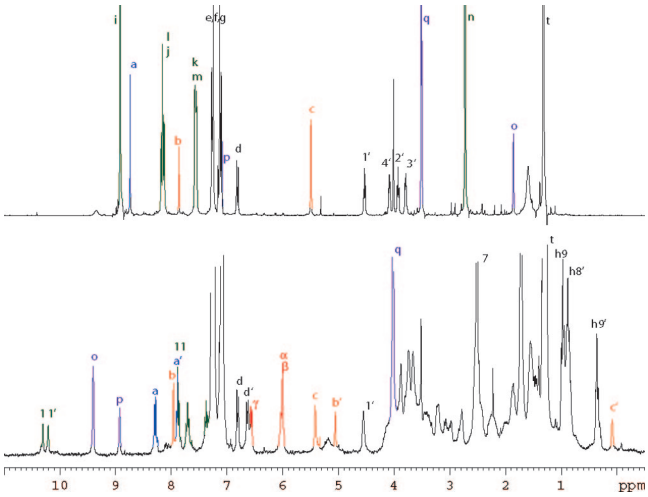

FIGURE 9. ^{1}H NMR spectra of a mixture of dumbbell **15** + 2 equiv of rhodium porphyrin **19** + pyridine **22** (top), and a mixture of rhodium rotaxane **21** plus pyridine ligand **22** (bottom).

Competitive binding by a potentially coordinating solvent provided one such possibility. However, addition of deuterated methanol or acetone resulted in no significant change in the porphyrin rotaxane, ^{1}H NMR spectra indicating that the triazole remained fully coordinated in these solvents. (Lack of solubility precluded use of other common potentially coordinating deuterated solvents.)

An alternative is the use of acid to protonate the triazole and hence prevent its coordination to the metal ion. However, control experiments on **19**⊃**18** established that, even in the presence of up to 30 equiv of TFA in a $CDCl_3$ solution, the coordinated triazole is not displaced.

Competitive ligand binding by stronger pyridine-based ligands was a third option. We could demonstrate that the pyridine ligand **22** was able to effectively and rapidly displace the triazole-coordinated dumbbell from a mixture of dumbbell **15** and 2 equiv of rhodium iodide tetratolyl porphyrin **19**.

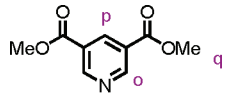

22

Addition of the pyridine ligand **22** resulted in the immediate decomplexation and rupture of the triazole−rhodium bond as evidenced by the appearance in the ^{1}H NMR spectrum of unbound dumbbell resonances (Figure 9). At the same time, new resonances for coordinated ligand **22** appeared at 7.15 and 1.86 ppm, which is characteristic of coordination of this ligand to rhodium porphyrins.[34]

However, upon addition of this ligand to a solution of the rotaxane **21**, no evidence for the disruption of the binding of the triazole to the rhodium porphyrin was observed, even at high or low temperatures. It is evident that in this case the effective intramolecular binding mode of the triazole in the rotaxane structure of **21** out-competes the exogenous ligand **22**.

However, when the stronger ligand pyridine itself was used in a competition experiment with the rotaxane, the proton spectra showed a new doublet appearing at 0.34 ppm, which displayed characteristic pyridine COSY patterns coupling to protons at 3.76 and 4.40 ppm. This strongly suggested that the pyridine had successfully displaced the coordinated triazole; however, variable temperature studies showed that, as the temperature decreased, the pyridine proton resonance shifted upfield. This is not characteristic behavior of pyridine binding to rhodium porphyrins, which is typically in slow exchange, and therefore temperature changes normally result in changes in peak intensity and not shifts in the peak position. In addition to this, no typical unbound triazole peaks were evident in the ^{1}H NMR spectrum, indicating either that the triazole moiety was still coordinated to the rhodium porphyrin or that it was not coordinated but still under the strap of the porphyrin. Similarly, no characteristic bound diimide peak was observed as might be expected if the pyridine was coordinated to the outside face of the porphyrin, which would allow diimide to bind in the cavity of the strapped porphyrin.

Clearly, the system was far from straightforward, and it was thought that, as in previous studies, the spectra may resolve over time as exchange of the pyridine ligand from inside to outside coordination modes may occur.[34] Unfortunately, over time, it appeared that the rotaxane was decomposing, as TLC analysis showed that the rotaxane had degraded into multiple porphyrin and nonporphyrin entities. This behavior was unexpected, as previous binding studies of rhodium porphyrin−pyridine complexes showed no such decomposition.[34] Nevertheless, this precluded a full investigation of the process, and unfortunately, it also suggests that the use of this rhodium porphyrin, despite showing promise, may not produce a stable rotaxane that is capable of controlled and reversible switching, at least with this combination of components.

Pyridine-Templated Rotaxanes via Click Methodology. Since the *diimide*/triazole combination in the thread was not conducive to a simple switching process, the click methodology was adapted to produce a *pyridine*/triazole thread alternative, based on the templating concepts described in the first sections of this paper. The pyridine azide **23** provided a suitable template.

Huisgen 1,3-dipolar cycloaddition between **23** and stopper alkyne **8** produced dumbbell **24** in reasonable yield (Scheme 4).

When the reaction was repeated in the presence of rhodium chloride strapped porphyrin **1** (as discussed previously, this particular rhodium porphyrin derivative was chosen, as derivatives of pyridine thread **23** have shown preferential inside coordination, which persists for up to 3 days at ambient temperature), the ^{1}H NMR spectrum of the major rhodium porphyrin product showed clear resonances for bound pyridine protons at 6.09 and 1.74 ppm and the expected integration for a 1:1 complex between rhodium porphyrin macrocycle **1** and pyridine dumbbell **24**. However split *meso* proton resonances at 10.29 and 9.88 ppm, as well as dual hexyl and methyl side chain peaks, and a single set of peaks for the strapped porphyrin naphthalene aromatic protons (7.01, 6.18, and 5.25 ppm) are not consistent with a rotaxane structure, but rather with one in which the central pyridine is coordinated on the same side of the porphyrin as the strap, but is not interlocked through it, as seen in the first section of this paper in the attempted rotaxane formation via acid chloride reactions.

Furthermore, addition of pyridine to this complex showed complete dissociation of the dumbbell **24** from the rhodium porphyrin due to competitive binding of the stronger ligand to the rhodium porphyrin. This indicates that the two components are indeed *not* mechanically linked as a rotaxane, but that the product is simply a strongly coordinatively bound complex. Indeed, the two components (the free dumbbell **24** and the

SCHEME 4

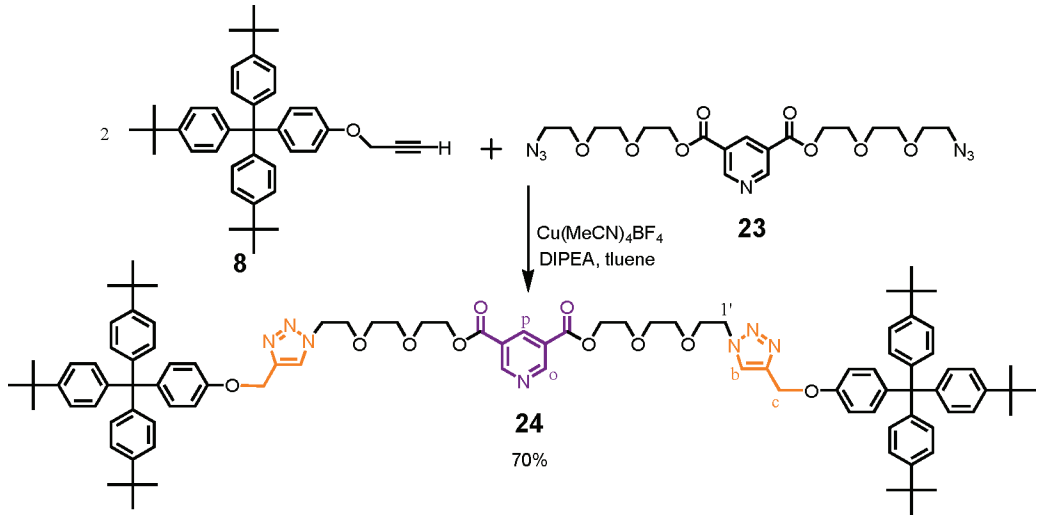

rhodium−pyridine complex) could be separated by preparative TLC in the presence of coordinating solvents, confirming that this mixture was not rotaxane. Thus, as for the acid chloride reactions, folding of the flexible strap of the porphyrin has effectively confounded the production of interlocked molecules by these templating strategies.

Conclusions

Unfortunately, the pyridine-directed template synthesis of supramolecular systems incorporating strapped porphyrin macrocycles has proved problematic. Despite optimizing conditions such that the ligands were bound preferentially inside the strap of the porphyrin, attempts to produce rotaxanes using a variety of reaction conditions were unsuccessful. Frustratingly, all attempts thus far at rotaxane formation using the pyridine templating resulted in the folding of the strap of the porphyrin so that no interlocked species were formed.

An alternative approach making use of the Cu(I)-catalyzed Huisgen 1,3-dipolar cycloaddition reaction (click chemistry) was successful in the production of triazole/diimide rotaxanes in relatively good yields. Of particular relevance is the strapped porphyrin rotaxane **17**, which is the first successful synthesis of a rotaxane incorporating this host and a diimide guest. In the zinc derivative of this rotaxane, the diimide unit is preferentially bound underneath the strap of the porphyrin. Conversely, for the corresponding rhodium(III) iodide analogue, the triazole entities are coordinated to the Rh(III) ion underneath the strap, and the diimide was displaced from the cavity. Unfortunately, this is not reversible, and no conditions were found that could create controlled, reversible "switching" for this rotaxane.

Nevertheless, the results presented here have demonstrated the potential of this type of click chemistry for the templated synthesis of a variety of rotaxanes or other interlocked molecules. Despite the drawbacks encountered in this work for the use of ligand templating methodologies for the production of interlocked metalloporphyrin supramolecular systems, we believe that, with appropriate adjustments to the templating ligand, the metal ion, and the superstructured porphyrin, the strategy can be successful and will be the subject of ongoing research.

Experimental Section

General. The synthesis of the unstrapped rhodium(III) iodide porphyrin **19** and the zinc and rhodium(III) chloride naphthoquinol strapped porphyrins (**9** and **1**, respectively) has been previously reported.[30,33,34,45] The pyridine thread **2**,[34] crown **14**,[41] and diimide **12**[46] were synthesized according to literature procedures. The stopper alkyne **8** was synthesized according to published procedures by Leigh.[37]

3-(2-(2-(2-Hydroxyethoxy)ethoxy)ethyl) 5-(2-(2-(10-oxo-10-(3-(10,15,20-tri-*p*-tolylporphyrin-5-yl)phenoxydecanoyloxy)ethoxy)-ethyl)pyridine-3,5-dicarboxylate (5). Sebacic acid tetratolyl porphyrin **3**[47] (210 mg, 0.25 mmol) was dissolved in excess oxalyl chloride (5 mL), and the mixture was stirred at room temperature under N_2 for 2 h. The reaction mixture was then pumped dry, solubilized in $CHCl_3$ (1 mL), and pumped dry. This procedure was repeated four times to remove all excess oxalyl chloride. The produced acid chloride porphyrin **4** (quantitative yield) in dry $CHCl_3$ (10 mL) was then added dropwise over 30 min to a solution of excess pyridine thread **2** (600 mg, 1.38 mmol) in dry $CHCl_3$ (30 mL). The reaction mixture was then stirred at room temperature under N_2 for 48 h. After this time, the mixture was diluted with $CHCl_3$ (30 mL) and washed with $NaHCO_3$ (saturated aqueous, 20 mL) and H_2O (20 mL). The crude product was purified by chromatotron (2 mm silica plate) using CH_2Cl_2/5%MeOH as the eluent before final crystallization from CH_2Cl_2/MeOH to yield the pure product **5** as a purple solid (175 mg, 56%): mp 128−130 °C; *m/z* (ESI-MS) $[M+H]^+$ 1270.5764 $C_{76}H_{80}N_5O_{13}$ (calcd 1270.5674); ^{1}H NMR (300 MHz, $CDCl_3$) δ 9.39 (2H, s, py *ortho* H), 8.88 (9H, m, Ar−H, py *para* H), 8.11 (7H, m, Ar−H), 7.99 (1H, s, Ar−H), 7.76 (1H, t, J = 7 Hz, Ar−H), 7.56 (7H, m, Ar−H), 4.51−4.55 (4H, m, OCH_2), 4.18−4.21 (2H, m, OCH_2), 3.82−3.84 (4H, m, OCH_2), 3.58−3.71 (14H, m, OCH_2), 2.73 (9H, s, CH_3), 2.64−2.68 (2H, m, CH_2), 2.27−2.32 (2H, m, CH_2), 1.81 (2H, m, CH_2), 1.61 (2H, m, CH_2), 1.33−1.41 (8H, m, CH_2), −2.76 (2H, s, NH); ^{13}C NMR (75 MHz, $CDCl_3$) δ 173.7, 172.4, 164.4, 154.3, 149.3, 144.7, 139.2, 138.2, 137.4, 134.5, 132.1, 131.2, 127.9, 127.4, 126.0, 120.9, 120.5, 120.3, 118.3, 72.5, 70.7, 70.6, 70.4, 69.3, 69.0, 64.8, 63.2,

(45) Wayland, B. B.; van Voorhees, S. L.; Wilker, C. *Inorg. Chem.* **1986**, *25*, 4039–4042.
(46) Hamilton, D. G.; Feeder, N.; Teat, S. J.; Sanders, J. K. M. *New J. Chem.* **1998**, 1019–1021.
(47) Johnstone, K. D. Self-Assembling Porphyrin Supramolecules. PhD Thesis, University of New England, Armidale, 2004.
(48) Ashton, P. R.; Ballardini, R.; Balzani, V.; Belohradsky, M.; Gandolfi, M. T.; Philp, D.; Prodi, L.; Raymo, F. M.; Reddington, M. V.; Spencer, N.; Stoddart, J. F.; Venturi, M.; Williams, D. J. *J. Am. Chem. Soc.* **1996**, *118*, 4931–4951.

61.8, 45.8, 34.5, 34.1, 29.1, 24.9, 21.5; UV (λ, nm (ε M^{-1} cm^{-1}), CH_2Cl_2) 419 (3.70×10^5), 515 (1.74×10^4), 551 (8.77×10^3), 591 (5.44×10^3), 646 (4.38×10^3).

2,7-Bis(2-(2-(2-(2-azidoethoxy)ethoxy)ethoxy)ethyl)benzo[*lmn*][3,8]phenanthroline-1,3,6,8(2*H*,7*H*)-tetraone (7). 2,7-Bis(2-(2-(2-(2-(4-toluenesulfonyl)ethoxy)ethoxy)ethoxy)ethyl)benzo[*lmn*][3,8]phenanthroline-1,3,6,8(2*H*,7*H*)-tetraone[49] (1.12 g, 1.21 mmol) and NaN_3 (1.56 g, 24.0 mmol) were suspended in dry, degassed DMF (30 mL). The mixture was stirred under N_2 at room temperature for 4 days before being diluted with H_2O (100 mL) and extracted with CH_2Cl_2 (3×60 mL). The organic layers were combined and washed with brine (100 mL) and dried over anhydrous Na_2SO_4, and the solvent was removed in vacuo. The compound was purified by chromatotron (2 mm silica plate) using 5% MeOH/CH_2Cl_2 as the eluent to give the pure product as an orange solid (671 mg, 83%): mp 57−59 °C; *m*/*z* (ESI-MS) $[M + Na]^+$ 691.2422 $C_{30}H_{36}N_8O_{10}Na$ (calcd 691.2452); ^1H NMR (300 MHz, $CDCl_3$) δ 8.59 (4H, s, NDI-H), 4.34−4.37 (4H, m, OCH_2), 3.76−3.79 (4H, m, OCH_2), 3.63−3.64 (4H, m, OCH_2), 3.53−3.58 (16H, m, OCH_2), 3.26−3.29 (4H, m, N_3CH_2); ^{13}C NMR (75 MHz, $CDCl_3$) δ 162.6, 130.8, 126.4, 70.6, 70.5, 70.0, 69.9, 67.7, 50.6, 39.5.

2,7-Bis(2-(2-(2-(2-(4-((4-(tris(4-*tert*-butylphenyl)methyl)-phenoxy)methyl)-1*H*-1,2,3-triazol-1-yl)ethoxy)ethoxy)ethoxy)-ethyl)benzo[*lmn*][3,8]phenanthroline-1,3,6,8(2*H*,7*H*)-tetraone (10). Naphthodiimide azide **7** (13 mg, 0.02 mmol), 4,4′,4″-((4-(prop-2-ynyloxy)phenyl)methanetriyl)tris(*tert*-butylbenzene) **8**[37] (23 mg, 0.04 mmol), *N*,*N*-diisopropylethylamine (DIPEA, 6 mg, 0.05 mmol), and $Cu(MeCN)_4BF_4$ (2 mg, 0.006 mmol) were dissolved in dry degassed toluene (5 mL), and the mixture was stirred under N_2 for 4 days. The reaction mixture was then diluted with H_2O (20 mL) and extracted with CH_2Cl_2 (30 mL). The organic layer was dried over anhydrous Na_2SO_4, and the solvent was removed. The product was purified by chromatotron (2 mm silica plate) using CH_2Cl_2/3% MeOH as the eluent and then crystallized from CH_2Cl_2/MeOH to give the pure product as a pale yellow solid (31 mg, 90%): mp 197−198 °C; *m*/*z* (ESI-MS) $[M + H]^+$ 1753.9776 $C_{110}H_{129}N_8O_{12}$ (calcd 1753.9730); ^1H NMR (300 MHz, $CDCl_3$) δ 8.73 (4H, s, NDI-H), 7.84 (2H, s, triazole H), 7.19−7.31 (16H, m, Ar−H), 7.09−7.16 (12H, m, Ar−H) 6.88 (4H, d, $J = 6$ Hz, OAr-H), 5.19 (4H, s, OCH_2−triazole), 4.54−4.57 (4H, m, CH_2−triazole), 4.46−4.48 (4H, m, NDI-CH_2), 3.83−3.90 (8H, m, OCH_2), 3.69−3.72 (4H, m, OCH_2), 3.57−3.61 (12H, m, OCH_2), 1.33 (54H, s, *t*-Bu); ^{13}C NMR (75 MHz, $CDCl_3$) δ 162.8, 156.2, 148.4, 144.1, 140.1, 132.3, 131.0, 130.7, 126.6, 124.0, 123.9, 113.3, 70.6, 70.5, 70.1, 69.4, 67.8, 63.1, 62.0, 50.3, 39.6, 34.3, 31.4.

4,4′,4″-((4-(2-(2-Azidoethoxy)ethoxy)phenyl)methanetriyl)tris(*tert*-butylbenzene) (13). 4,4′,4″-((4-(2-(2-(4-Toluenesulfonyloxy)-ethoxy)ethoxy)phenyl)methanetriyl)tris(*tert*-butylbenzene)[48] (0.99 g, 1.32 mmol) and NaN_3 (0.86 g, 13.2 mmol) were suspended in dry, degassed DMF (10 mL). The mixture was stirred under N_2 at room temperature for 3 days before being diluted with H_2O (50 mL) and extracted with CH_2Cl_2 (3×50 mL). The organic layers were combined and washed with brine (50 mL) and dried over anhydrous Na_2SO_4, and the solvent was removed in vacuo. The compound was purified by chromatotron (2 mm silica plate) using 20% hexane/CH_2Cl_2 as the eluent to give the pure product as a white solid (513 mg, 63%): mp 208−210 °C; *m*/*z* (FAB-MS) $[M + H]^+$ 617.3991 $C_{41}H_{52}N_3O_2$ (calcd 617.3981); ^1H NMR (300 MHz, $CDCl_3$) δ 7.25−7.28 (6H, m, Ar−H), 7.10−7.13 (8H, m, Ar−H), 6.82 (2H, d, $J = 6$ Hz, OAr-H), 4.14−4.17 (2H, m, OCH_2), 3.87−3.90 (2H, m, OCH_2), 3.76−3.79 (2H, m, OCH_2), 3.42−3.45 (2H, m, N_3CH_2), 1.34 (27H, s, *t*-Bu); ^{13}C NMR (75 MHz, $CDCl_3$) δ 156.5, 148.3, 144.2, 139.9, 132.4, 130.8, 124.1, 113.2, 70.3, 69.9, 67.3, 63.1, 50.8, 34.4, 31.5.

2,7-Bis((1-(2-(2-(4-(tris(4-*tert*-butylphenyl)methyl)phenoxy)-ethoxy)ethyl)-1*H*-1,2,3-triazol-4-yl)methyl)benzo[*lmn*][3,8]-phenanthroline-1,3,6,8(2*H*,7*H*)-tetraone (15). 2,7-Di(prop-2-ynyl)benzo[*lmn*][3,8]phenanthroline-1,3,6,8(2*H*,7*H*)-tetraone **12**[46] (8 mg, 0.025 mmol), 4,4′,4″-((4-(2-(2-azidoethoxy)ethoxy)phenyl) methanetriyl)tris(*tert*-butylbenzene) **13** (30 mg, 0.05 mmol), DIPEA (6 mg, 0.05 mmol), and $Cu(MeCN)_4BF_4$ (2 mg, 0.006 mmol) were dissolved in dry degassed toluene (5 mL), and the mixture was stirred under N_2 for 8 days. The reaction mixture was then diluted with H_2O (20 mL) and extracted with CH_2Cl_2 (30 mL). The organic layer was dried over anhydrous Na_2SO_4, and the solvent was removed. The product was purified by crystallization from CH_2Cl_2/MeOH to give the pure product as a pale yellow solid (32 mg, 80%): mp 204−207 °C; *m*/*z* (ESI-MS) $[M + H]^+$ 1577.8690 $C_{102}H_{113}N_8O_8$ (calcd 1577.8681); ^1H NMR (300 MHz, $CDCl_3$) δ 8.74 (4H, s, a), 7.87 (2H, s, b), 7.24−7.29 (12H, m, g), 7.09−7.16 (16H, m, e,f) 6.80 (4H, d, $J = 6$ Hz, d), 5.50 (4H, s, c), 4.52−4.55 (4H, m, 1′), 4.07−4.10 (4H, m, 4′), 3.91−3.95 (4H, m, 2′), 3.79−3.81 (4H, m, 2′), 1.32 (54H, s, t); ^{13}C NMR (75 MHz, $CDCl_3$) δ 162.4, 156.4, 148.4, 144.1, 142.7, 140.1, 132.3, 131.2, 130.7, 126.8, 136.6, 124.5, 124.1, 113.1, 69.9, 69.6, 67.1, 63.1, 50.3, 35.6, 34.3, 31.4.

Crown Rotaxane (16). 2,7-Di(prop-2-ynyl)benzo[*lmn*][3,8]phenanthroline-1,3,6,8(2*H*,7*H*)-tetraone **12**[46] (8 mg, 0.025 mmol), 4,4′,4″-((4-(2-(2-azidoethoxy)ethoxy)phenyl)methanetriyl)tris(*tert*-butylbenzene) **13** (30 mg, 0.05 mmol), dinaphtho-38-crown-10 **14** (16 mg, 0.025 mmol), and DIPEA (6 mg, 0.05 mmol) were dissolved in dry degassed toluene (5 mL), and the mixture was stirred under N_2 for 1 h to allow solubilization of the diimide. After this time, $Cu(MeCN)_4BF_4$ (2 mg, 0.006 mmol) was added, and the mixture was stirred at room temperature under N_2 for 3 days. The reaction mixture was then diluted with H_2O (20 mL) and extracted with CH_2Cl_2 (30 mL). The organic layer was dried over anhydrous Na_2SO_4, and the solvent was removed. The product was purified by chromatotron (2 mm silica plate) using 5% MeOH/CH_2Cl_2 as the eluent, yielding dumbbell **15** (18 mg, 46%) and crown rotaxane products. The crown rotaxane was then crystallized from EtOAC/hexane to give the pure crown rotaxane as a pale pink solid (22 mg, 43%); mp 181−184 °C; *m*/*z* (ESI-MS) $[M + H]^+$ 2214.1600 $C_{138}H_{157}N_8O_{18}$ (calcd 2214.1616); ^1H NMR (300 MHz, $CDCl_3$) δ 8.31 (4H, s, a), 8.08 (2H, s, b), 7.24−7.29 (12H, m, g), 7.08−7.11 (16H, m, e, f), 6.76−6.79 (8H, d, $J = 6$ Hz, d, γ), 6.26 (4H, t, $J = 8$ Hz, β), 5.90 (4H, d, $J = 6$ Hz, α), 5.41 (4H, s, c), 4.64−4.67 (4H, m, 1′), 3.99−4.07 (16H, m, OCH_2), 3.87−3.92 (24H, m, OCH_2), 3.78−3.81 (4H, m, OCH_2), 1.32 (54H, s, t); ^{13}C NMR (75 MHz, $CDCl_3$) δ 162.6, 156.3, 152.9, 148.4, 144.1, 143.2, 140.0, 132.3, 130.7, 125.5, 125.0, 124.7, 124.0, 123.5, 114.1, 113.1, 103.5, 77.2, 71.4, 71.2, 69.9, 69.8, 67.3, 67.1, 63.1, 50.4, 34.6, 34.3, 31.4; UV (λ, nm (ε M^{-1} cm^{-1}), CH_2Cl_2) 500 (745).

Zinc Porphyrin Rotaxane (17). 2,7-Di(prop-2-ynyl)benzo[*lmn*][3,8]phenanthroline-1,3,6,8(2*H*,7*H*)-tetraone **12**[46] (8 mg, 0.025 mmol), 4,4′,4″-((4-(2-(2-azidoethoxy)ethoxy)phenyl)methanetriyl)-tris(*tert*-butylbenzene) **13** (30 mg, 0.05 mmol), strapped porphyrin **9** (33 mg, 0.025 mmol), and DIPEA (6 mg, 0.05 mmol) were dissolved in dry degassed toluene (5 mL), and the mixture was stirred under N_2 for 1 h to allow solubilization of the diimide. After this time, $Cu(MeCN)_4BF_4$ (2 mg, 0.006 mmol) was added, and the mixture was stirred at room temperature under N_2 for 3 days. The reaction mixture was then diluted with H_2O (20 mL) and extracted with CH_2Cl_2 (30 mL). The organic layer was dried over anhydrous Na_2SO_4, and the solvent was removed. The product was purified by chromatotron (2 mm silica plate) using 2% MeOH/CH_2Cl_2 as the eluent, yielding dumbbell **15** (21 mg, 55%) and porphyrin rotaxane products. The porphyrin rotaxane was then crystallized from EtOAC/hexane to give the pure porphyrin rotaxane **17** as a purple solid (11 mg, 20%): mp 145−148 °C; *m*/*z* (ESI-MS) $[M]^+$ 2913.5612 $C_{184}H_{216}N_{12}O_{16}Zn$ (calcd 2913.5749); ^1H NMR (300 MHz, $CDCl_3$) δ 9.78 (2H, s, *meso*), 7.78 (2H, s, b), 7.70 (2H, t, $J = 7$ Hz, 13), 7.36 (2H, d, $J = 8$ Hz, 14), 7.25−7.29 (16H, m, e,

(49) Hansen, J. G.; Feeder, N.; Hamilton, D. G.; Gunter, M. J.; Becher, J.; Sanders, J. K. M. *Org. Lett.* **2000**, *2*, 449–452.

g), 7.09−7.16 (14H, m, f, 12), 6.94 (2H, t, J = 6 Hz, 11), 6.74 (4H, d, J = 6 Hz, d), 6.42 (4H, s, a), 5.86 (2H, d, J = 6 Hz, γ), 5.25 (2H, t, J = 8 Hz, β), 5.12 (4H, s, c), 4.87 (4H, m, 16), 4.66 (2H, d, J = 6 Hz, α), 4.46 (4H, m, 1′), 4.22 (4H, m, 17), 4.08 (4H, m, h4), 3.95 (4H, m, 4′), 3.80−3.85 (12H, m, h4, 19, 2′), 3.72 (4H, m, 18), 3.62 (4H, m, 3′), 3.54 (4H, m, 20), 3.29 (4H, m, 21), 2.58 (12H, s, 7), 2.14 (8H, m, h5), 1.76 (8H, m, h6), 1.45−1.57 (16H, m, h7, h8), 1.34 (54H, s, t), 0.92 (12H, m, h9); ^{13}C NMR (75 MHz, $CDCl_3$) δ 159.9, 157.8, 156.3, 151.9, 148.4, 148.1, 145.5, 144.1, 143.1, 142.8, 140.0, 137.9, 135.9, 132.8, 132.3, 130.7, 129.5, 126.9, 125.6, 124.1, 123.7, 122.6, 120.8, 120.6, 119.7, 115.4, 113.0, 110.7, 102.9, 96.2, 71.1, 70.3, 69.7, 69.6, 67.6, 67.1, 65.6, 63.1, 50.2, 34.3, 33.4, 32.0, 31.4, 30.1, 27.0, 22.7, 14.2; UV (λ, nm (ε M^{-1} cm^{-1}), CH_2Cl_2) 417 (2.48 × 10^5), 537 (1.57 × 10^4), 570 (9.76 × 10^3).

1-(2-(2-(4-(Tris(4-*tert*-butylphenyl)methyl)phenoxy)ethoxy)-ethyl)-4-((4-(tris(4-*tert*-butylphenyl)methyl)phenoxy)methyl)-1*H*-1,2,3-triazole (18). 4,4′,4″-((4-(Prop-2-ynyloxy)phenyl)methanetriyl)tris(*tert*-butylbenzene) **8**[37] (20 mg, 0.04 mmol), 4,4′,4″-((4-(2-(2-azidoethoxy)ethoxy)phenyl)methanetriyl)tris(*tert*-butylbenzene) **13** (23 mg, 0.04 mmol), DIPEA (5 mg, 0.04 mmol), and $Cu(MeCN)_4BF_4$ (1.2 mg, 0.004 mmol) were dissolved in dry degassed toluene (5 mL), and the mixture was stirred under N_2 for 4 days. The reaction mixture was then diluted with H_2O (20 mL) and extracted with CH_2Cl_2 (30 mL). The organic layer was dried over anhydrous Na_2SO_4, and the solvent was removed. The product was purified by chromatotron (2 mm silica plate) using CH_2Cl_2 as the eluent to give the pure product **18** as a white solid (30 mg, 71%): mp 264−265 °C; *m*/*z* (ESI-MS) $[M + H]^+$ 1160.7576 $C_{81}H_{98}N_3O_3$ (calcd 1160.7608); ^{1}H NMR (300 MHz, $CDCl_3$) δ 7.81 (1H, s, triazole), 7.21−7.24 (12H, m, Ar−H), 7.04−7.09 (16H, m, Ar−H), 6.73−6.80 (4H, m, OAr-H), 5.13 (2H, s, OCH_2−triazole), 4.56−4.60 (2H, m, OCH_2), 4.03−4.06 (2H, m, OCH_2), 3.94−3.97 (2H, m, OCH_2), 3.78−3.81 (2H, m, OCH_2), 1.30 (54H, s, t); ^{13}C NMR (75 MHz, $CDCl_3$) δ 156.3, 156.1, 148.3, 144.1, 140.1, 132.3, 130.7, 126.7, 113.3, 113.0, 69.9, 69.6, 67.0, 63.1, 61.9, 34.3, 31.4.

Rhodium Porphyrin Rotaxane (21). Free base porphyrin rotaxane **20** (13 mg, 0.005 mmol), anhydrous sodium acetate (4 mg, 0.05 mmol), and $[Rh(CO)_2Cl]_2$ (3 mg, 0.008 mmol) were dissolved in dry degassed DCM, and the reaction mixture was stirred at room temperature under N_2 for 5 h. Solid I_2 (4 mg, 0.02 mmol) was then added, and the mixture was stirred under N_2 overnight at room temperature. The solution was then diluted with CH_2Cl_2 (30 mL) and washed with saturated $KI_{(aq)}$ (20 mL) and H_2O (3 × 20 mL). The organic layer was dried over anhydrous Na_2SO_4 and the solvent removed in vacuo. The product was purified by preparative TLC (2 mm silica plate) using 2% MeOH/CH_2Cl_2 as the eluent. The product was then crystallized from EtOAC/hexane to give the pure porphyrin rotaxane **21** as a red solid (5 mg, 40%): mp 151−152 °C; *m*/*z* (ESI-MS) $[M + H]^+$ 3080.4540 $C_{184}H_{217}N_{12}O_{16}RhI$ (calcd 3080.4635); ^{1}H NMR (300 MHz, $CDCl_3$ at −20 °C) δ 10.30 (1H, s, 1), 10.21 (1H, s, 1′), 8.30 (2H, d, J = 8 Hz, a), 7.97 (1H, s, b), 7.86−7.90 (4H, m, a′, 11), 7.70 (2H, t, J = 7 Hz, 12), 7.36 (2H, t, J = 8 Hz, 13), 7.23−7.29 (16H, m, e, g), 7.07−7.15 (14H, m, f, 12), 6.81 (2H, d, J = 6 Hz, d), 6.63 (2H, d, J = 6 Hz, d′), 6.57 (2H, d, J = 6 Hz, γ), 6.01−6.04 (4H, m, β, α), 5.43 (2H, s, c), 5.02 (1H, s, b′), 4.56 (2H, m, 1′), 3.50−4.21 (24H, m, 16, 17, 20, 21, h4, h4′), 3.40 (4H, m, 2′, 3′), 3.20 (4H, m, 19), 2.90−3.11 (4H, m, 4″, 3″), 2.78 (4H, m, 18), 2.50 (16H, m, 7, 1″, 2″), 2.23 (8H, m, h5, h5′), 1.44−1.87 (20H, m, h6, h6′, h7, h7′, h8), 1.30 (54H, s, t, t′), 0.89−1.00 (10H, m, h9, h8′), 0.37 (6H, m, h9′), 0.11 (2H, s, c′); ^{13}C NMR (75 MHz, $CDCl_3$) δ 158.3, 156.3, 153.5, 148.4, 144.1, 143.6, 140.0, 136.3, 133.3, 132.3, 132.0, 130.7, 130.2, 129.7, 125.4, 124.0, 121.6, 114.9, 113.5, 113.3, 113.0, 105.6, 98.1, 70.5, 70.2, 69.5, 68.7, 68.0, 67.9, 66.9, 63.1, 34.3, 33.9, 32.1, 31.4, 30.1, 30.0, 29.8, 27.1, 22.7, 14.9, 14.1; UV (λ, nm (ε M^{-1} cm^{-1}), CH_2Cl_2) 423 (1.40 × 10^5), 534 (1.94 × 10^4), 564 (9.41 × 10^3).

Bis(2-(2-(2-azidoethoxy)ethoxy)ethyl) pyridine-3,5-dicarboxylate (23). Bis(2-(2-(2-hydroxyethoxy)ethoxy)ethyl) pyridine-3,5-dicarboxylate **2** (1.2 g, 2.74 mmol) and Et_3N (650 μL) were dissolved in dry $CHCl_3$ (40 mL) under N_2 and stirred in an ice/salt bath. 4-Toluenesulfonyl chloride (1.06 g, 5.6 mmol) and Et_3N (475 μL) in dry $CHCl_3$ were added dropwise over 30 min. The mixture was then refluxed under N_2 for 7 days before being diluted with cold water (100 mL). The organic layer was separated, washed with H_2O (100 mL), and dried over anhydrous Na_2SO_4, and the solvent was removed. The crude tosylate was then added to a suspension of NaN_3 in dry, degassed DMF (20 mL) and stirred at room temperature under N_2 for a further 4 days. The reaction mixture was again diluted with H_2O (100 mL) and extracted with CH_2Cl_2 (3 × 50 mL). The organic layers were combined and then washed with brine (50 mL) and dried over anhydrous Na_2SO_4, and the solvent was removed in vacuo. The product was purified by chromatotron (2 mm silica plate) using 2% MeOH/CH_2Cl_2 as the eluent to give the pure product as yellow oil (180 mg, 13%): *m*/*z* (FAB-MS) $[M + H]^+$ 482.2012 $C_{19}H_{28}N_7O_8$ (calcd 482.1999); ^{1}H NMR (300 MHz, $CDCl_3$) δ 9.39 (2H, s, py *ortho*-H), 8.89 (1H, s, py *para*-H), 4.54−4.57 (4H, m, OCH_2), 3.86−3.89 (4H, m, OCH_2), 3.67−3.71 (12H, m, OCH_2), 3.36−3.40 (4H, m, N_3CH_2); ^{13}C NMR (75 MHz, $CDCl_3$) δ 164.4, 154.3, 138.2, 126.0, 77.2, 70.7, 70.1, 69.1, 64.8, 50.7.

Bis(2-(2-(2-(4-((4-(tris(4-*tert*-butylphenyl)methyl)phenoxy)-methyl)-1*H*-1,2,3-triazol-1-yl)ethoxy)ethoxy)ethyl)pyridine-3,5-dicarboxylate (24). Propargyl ether **8**[37] (27 mg, 0.05 mmol), pyridine-3,5-dicarboxylic acid bis-(2-(2-(2-azidoethoxy)-ethoxy)-ethyl) ester **23** (12 mg, 0.025 mmol), DIPEA (6 mg, 0.05 mmol), and $Cu(MeCN)_4BF_4$ (2 mg, 0.005 mmol) were dissolved in dry degassed toluene (5 mL), and the mixture was stirred under N_2 for 2 days. The reaction mixture was then diluted with H_2O (20 mL) and extracted with CH_2Cl_2 (30 mL). The organic layer was then dried over anhydrous Na_2SO_4, and the solvent was removed. The product was purified by preparative TLC (2 mm silica plate) using 2% MeOH/CH_2Cl_2 as the eluent followed by recrystallization from EtOAc/hexane to give the pure product **24** as a white solid (25 mg, 70%): mp 207−209 °C; *m*/*z* (ESI-MS) $[M + H]^+$ 1566.9073 $C_{99}H_{120}N_7O_{10}$ (calcd 1566.9097); ^{1}H NMR (300 MHz, $CDCl_3$) δ 9.40 (2H, s, py *ortho*-H), 8.89 (1H, s, py *para*-H), 7.80 (2H, s, triazole), 7.23−7.26 (12H, m, Ar−H), 7.10−7.13 (16H, m, Ar−H), 6.87 (4H, d, J = 6 Hz, OAr-H), 5.19 (4H, s, OCH_2−triazole), 4.51−4.57 (8H, m, OCH_2), 3.89−3.92 (4H, m, OCH_2), 3.78−3.81 (4H, m, OCH_2), 3.64 (8H, m, OCH_2), 1.32 (54H, s, t); ^{13}C NMR (75 MHz, $CDCl_3$) δ 164.3, 156.2, 154.3, 148.4, 144.2, 140.2, 132.3, 130.7, 124.0, 123.8, 113.3, 70.6, 69.5, 69.0, 64.7, 63.1, 62.0, 50.3, 34.3, 31.4.

Acknowledgment. This research was supported by the Australian Research Council.

Supporting Information Available: General experimental procedures and 1D spectra for new compounds. Binding constant determination for **12** with **19**. UV−vis absorption spectrum of **16**. ^{1}H NMR comparison of **18** and **18** plus **19**. Relevant 2D NMR and mass spectral data for interlocked structures. This material is available free of charge via the Internet at http://pubs.acs.org.

JO800276W